Measurements of Small Scale Turbulence in an Axisymmetric Jet Using Moving Hot-wires

Hussein J. Hussein
Department of Mechanical Engineering
Vanderbilt University
Nashville, TN 37235

and

William K. George
Turbulence Research Laboratory
University at Buffalo, SUNY
Buffalo, N.Y. 14260

April 27, 1991

ABSTRACT

The fine scale characteristics of turbulent flow resulting from an axisymmetric jet exhausting into a quiescent environment is investigated. Measurements are carried out in the far field of the jet with exit Reynolds numbers of 10^5. Moments of the velocity and mean-square derivatives of the velocity field are obtained using flying hot-wire anemometry.

The measured derivative correlations are used to test the conditions for the requirements of local-isotropy. It is found that the relative magnitudes of the measured mean-square derivative correlations are better described by the relations for axisymmetric homogeneous turbulence. Results of the velocity moments and the rate of dissipation of kinetic energy are presented. Comparisons of the results of flying hot-wire errors with those from laser Doppler anemometry and stationary hot wire probes are used to assess hot-wire cross-flow and rectification errors for high turbulence intensity flows.

TABLE OF CONTENTS

1. Introduction

The present work consists of an extensive investigation of an axisymmetric turbulent jet using flying hot-wire probes. The overall objective is to provide a basis for evaluating turbulence closure hypotheses from measurements of the moments of the velocity and the rate of dissipation of turbulence energy. The secondary objectives are: a direct measurement of the dissipation, an evaluation of hot-wire errors in this high turbulence intensity flow, and an evaluation of prior LDA data.

The high turbulence intensity in a jet gives rise to cross-flow and rectification errors on hot-wires (Tutu and Chevray 1975). These errors as well as the effect of the fluctuating convection velocity on the measured derivatives can be reduced by superimposing a velocity on the hot-wire, thereby reducing the effective turbulence intensity. This was accomplished by using hot-wires mounted on a rotating wing which reduced the effective turbulence intensity from 30% to 11% at the centerline of the jet and to a maximum of 38% at the outer edge.

Measurements of the dissipation in the past always relied on the assumption of Taylor's frozen field hypothesis and the assumption of local isotropy. The former is known to fail in high turbulence intensity flows while the latter has never been confirmed experimentally in laboratory shear flows. In this experiment, spatial velocity derivatives were measured using parallel single-wires and a new AXI-probe which consisted of 1 - 1/2 x-wires. The superposition of a mean velocity on the wires enabled both the evaluation of the effects of turbulence intensity on Taylor's hypothesis, and the use of this hypothesis to obtain the velocity derivative in the streamwise direction. The derivative measurements showed that the flow could not be considered locally isotropic, but did satisfy the derivative relations for axisymmetric homogeneous turbulence.

2. Governing equations for the dissipation and kinetic energy

Momentum equation

The momentum equation of incompressible isothermal steady state turbulent flow is obtained from the Navier-Stokes equations. For an axisymmetric jet with no swirl the turbulent shear stresses $\langle u_1 u_3 \rangle$ and $\langle u_2 u_3 \rangle$ are zero, the azimuthal component of the velocity field U_3 is also zero. The equations governing the mean velocity are:

$$U\frac{\partial U}{\partial x} + V\frac{\partial U}{\partial r} = -\frac{1}{\rho}\frac{\partial P}{\partial X} - \frac{1}{r}\frac{\partial(-r\langle uv\rangle}{\partial r} - \frac{\partial\langle u\rangle^2}{\partial x} \qquad (1)$$

$$U\frac{\partial V}{\partial x} + V\frac{\partial V}{\partial r} = -\frac{1}{\rho}\frac{\partial P}{\partial x} - \frac{1}{r}\frac{\partial(-r\langle v\rangle^2)}{\partial r} - \frac{1}{r}\frac{\partial(-r\langle uv\rangle}{\partial x} + \frac{\langle w\rangle^2}{r} \qquad (2)$$

The velocity and lengths in the above scale as,

$$\frac{\partial U}{\partial x} \sim \frac{U}{L}$$

$$\frac{\partial}{\partial r} \sim \frac{1}{\delta}$$

For a jet issuing into a quiescent environment assuming a thin shear layer approximation $\delta/L \ll 1$, equations 1 and 2 the following first order momentum equation is obtained.

$$U\frac{\partial U}{\partial x} + V\frac{\partial U}{\partial y} = -\frac{1}{r}\frac{\partial r\langle uv\rangle}{\partial r} - \frac{1}{\rho}\frac{\partial P}{\partial x}$$

$$\frac{P_\infty}{\rho} - \frac{P}{\rho} = -\int_r^\infty \frac{\partial \langle u\rangle^2}{\partial r}\partial r - \int_r^\infty \left[\frac{\langle v\rangle^2 + \langle w\rangle^2}{r}\right]$$

the continuity equation is,

$$\frac{\partial U}{\partial x} + \frac{1}{r}\frac{\partial (rV)}{\partial r} = 0$$

The validity of the measured data can be verified by utilizing the integrated form of above equations (see section 4.2).

The interest in measuring the terms in the momentum equations stem from the classical problem of the turbulence equations being an unclosed set of equations. The aim of modelers is to determine the mean velocity from the above momentum equations. Because of the presence of the Reynolds stress there are more unknowns than equations making it necessary to find a way of closing the equations.

Reynolds stress equations

The transport equations for the Reynolds stresses are:

$$\frac{D\langle u_i u_j\rangle}{Dt} = -\frac{\partial}{\partial x}\left[\langle u_i u_j u_k\rangle + \frac{\langle p u_i\rangle}{\rho}\delta_{jk} + \frac{\langle p u_j\rangle}{\rho}\delta_{ik} - \nu\frac{\partial\langle u_i u_j\rangle}{\partial x_k}\right]$$

$$-\langle u_i u_k\rangle\frac{\partial U_i}{\partial x_k} - \langle u_j u_k\rangle\frac{\partial U_i}{\partial x_k} + \frac{P}{\rho}\left\langle\frac{\partial u_i}{\partial x_j} + \frac{\partial u_i}{\partial x_i}\right\rangle - \frac{2}{3}\epsilon\delta_{ij}$$

For high Reynolds number flow the viscous diffusion term is negligible. The third moments which represent the diffusion by the turbulent velocity fluctuations, $\langle u_i u_j u_k\rangle$, are modeled in terms of the Reynolds stress terms. The terms containing the diffusion of pressure correlations, $\langle p u_k\rangle$ are also modeled in terms of velocity correlations, Lumley (1978). The pressure-strain correlations $p\langle\partial u_i/\partial x_j + \partial u_i/\partial x_j\rangle/\rho$ are modeled in terms of an anisotropic stress tensor which can be related to the Reynolds stress.

In evaluating these models it is advantageous to measure as man terms as possible in the above equation which makes it crucial to measure the dissipation term directly. This direct measurement of the dissipation can be a cornerstone in the evaluation of the quality of these models.

Kinetic energy equation

The equation for the transport of the kinetic energy is given by

$$\frac{Dk}{Dt} = -\frac{\partial}{\partial x_k}\left[\frac{1}{2}\langle q^2 u_k\rangle + \frac{\langle p u_k\rangle}{\rho} - \nu\frac{\partial k}{\partial x_k} - \langle u_i u_j\rangle\frac{\partial U_i}{\partial x_j}\right] - \epsilon$$

All the terms in the above equation except the pressure transport term (which is modeled) can be measured. Earlier investigators (Taulbee et al 1987) used the dissipation as a closing term. Measuring the dissipation directly, provides the data necessary to evaluate the terms involving the pressure.

3. Experimental facility and measurement hardware

3.1 The jet facility

The jet apparatus was the same one utilized by Capp (1983) (see also Taulbee et al. 1987), for which the measured velocity profile at the exit had a velocity overshoot at the jet edges of 3% relative to the centerline velocity. This effect was balanced by the boundary layer thickness (approximately 2% of the exit radius). The error term in the momentum integral arising from the adoption

of a top hat profile based upon the centerline velocity and the exit diameter is less than 3%. The exit conditions listed in Table I were used for all experimental measurements reported here.

3.2 The enclosure

While the jet apparatus shown on Figure 1, was the same as used by Capp (1983), the enclosure was different. In this experiment the apparatus was used in the large 5m x 5m x 25m room utilized in the measurements of Taulbee et al. (1987). The size of the room was determined using the criterion proposed by Capp (1983) (see also George et al. 1986) to ensure that the momentum integral was constant to within 5% at 150 diameters. The jet was mounted on a table 2.5m above the floor to place the exit near the geometrical center of the room cross-section. The temperature of the room was monitored throughout the experiment and was constant to within $\pm$ 3°C.

The axisymmetry of the jet was very carefully documented. A three dimensional traversing system designed for this experiment was utilized to obtain velocity contours which show excellent axisymmetry. The collapse of the profiles when scaled with the centerline velocity and downstream distance indicates a well established similarity region. The virtual origin of the jet was found to be 2.7 diameters from the exit. The measurements reported here were taken at only 70 and 100 diameters downstream of the jet exit in the stationary probe experiment, and 70 diameters downstream with the moving probe.

3.3 Flying hot-wire anemometry

Flying hot wires in turbulent flows were used in the past by various investigators. Uberoi (1975) used a flying wire in his study of entrainment in shear flows. Cantwell & Coles (1983), Watmuff et al. (1983), Panchapakesan and Lumley (1986, 1987) are other investigators that applied the moving wire techniques in a wind-tunnel, wake and a heated jet respectively. There are various reasons why the moving wires were used. In this work the objective is two-fold; to decrease the errors due to cross-flow and rectification, and to enable a correct implementation of Taylor's hypothesis. These particular advantages of a moving probe appear to have first been noted by George and Beuther (1979).

The moving wire experiments were performed by whirling the probes about an axis perpendicular to the axis of the jet. To decrease the interference of the supporting arm, the probes were mounted on a one meter long, low drag symmetric NACA 0010 airfoil. A one horse-power motor was used in combination with a set of reduction gears and counter weights to obtain a smooth rotation of the wing. The entire mechanism was mounted on a one dimensional manual traversing system which was used to traverse the probes across the jet. A sketch of the apparatus is shown in Figure 2.

The effect of the wing on the flow was carefully studied. The wing had a low coefficient of drag C_d of 0.0045 and a Reynolds number of 1700 at 1 m/s. The large scale characteristics of the flow around the moving wing were observed with smoke wires. The results showed minimal amounts of flow disturbances on the jet

as the wing rotated through it.

The data were collected only when the probe was parallel to the axis of the jet. This was accomplished by using an encoder pulse that triggered the A/D converter to collect data. The short charging time of the sample and hold of the A/D (nanoseconds) insured that the measurement was effectively taken at a point. One data sample was collected for each revolution and 4800 samples were taken at each radial position.

The hot-wire signal was transmitted from the probes to the anemometers using low noise slip-rings. The slip-rings were enclosed in a grounded aluminum housing so as to avoid stray electromagnetic noise. The coaxial cables connecting the slip-rings to the anemometers were also shielded. The noise due to the slip-rings was estimated to be of the order of 1 mV. Both the original velocity signal and it's time derivative were recorded for each of the wires.

3.4 Measurement procedure of the velocity derivatives

The measurements of the spatial derivatives were done by measuring the velocity components at two points that are in close proximity to each other, and taking the difference to approximate the velocity gradient. The noise in the difference signal is due to either quantization and electronic noise or to uncertainty in the calibration of the two wires. The voltage to velocity transformation is accurate to within 0.1%, the quantization error is of the order of 0.6 mv, and rms electronic noise is of the order of 3 mv. A conservative estimate of the error in the measured mean square derivatives from these sources is less than 10%.

3.5 Experimental procedure

Data acquisition and sampling considerations:

The hot-wire signals were digitized using a 15 bit, 16 channel A/D converter with a throughput rate of 150 kHz. The anti-aliasing filters used were Bessel Low-Pass Filters (manufactured by Frequency Devices, Model 848 P8195) and were tunable over a frequency range of 200 Hz to 51.2 kHz.

Measurements of all of the components of the velocity were made and all the moments to the fourth order were computed. Care was taken to ensure that record lengths were long enough to ensure that statistical convergence was achieved, and that the dynamical ranges were adequate to minimize adversely affecting the higher moments by clipping the tails of the probability distributions.

The streamwise gradients of the velocity components were computed from Taylor's hypothesis using the time derivative of the velocity and the local mean velocity. The former was obtained by substituting the time derivative of the anemometer output into the derivative of the wire calibration. The differentiation of the electronic signal was accomplished by utilizing the high-pass filter characteristics of the Dantec 55D26 signal conditioning unit. It is well-known that differentiation corresponds to +6 dB/octave frequency response function which is also the low frequency asymptote of a single-pole high pass

filter. To ensure that the deviations from this asymptote near the breakpoint were negligible, the high pass cut-off frequency was chosen about five times higher than the highest frequency of interest in the signal, that corresponding to the Kolmogrov microscale. For the moving probe experiment this corresponds to a high frequency cut-off of 65 kHz.

Description of hot-wire probes:

The two different types of hot-wire probes used in this work were a standard parallel wire probe and a three wire probe that was designed for these experiments. All the wires used on the probes were Wollaston (Pt-10%Rh) with 2.5 micron diameter. Since the wires originally had a silver coating, a sensing element 0.2mm long was etched by a nitric acid solution. Compared to the Kolmogorov scales in this flow which are about 0.16mm at the centerline of the jet, the wires were sufficiently short so that the variances of the measured derivatives were not affected by length effects ($l_w < \pi\eta$ where η is the Kolmogorov microscale, Wyngaard 1968). The small diameter of the wires was chosen since smaller diameter wires have higher resistance and hence better signal to noise ratio (Doughman 1972).

The anemometers used were Dantec 55M constant temperature anemometers operated with 0.6 overheat ratio. To avoid aliasing of the signals, signal conditioners were used to low pass the signals. The highest frequency in the flow (corresponding to the Kolmogorov microscale) was 12 kHz, so the low pass setting for the filters was at 15 Khz. This cutoff frequency was calculated using the sum of jet velocity and superimposed velocity as the convection velocity.

The parallel wire probe shown on Figure 3 was used in two different experiments. The first experiment was performed with the probe oriented in such a way as to measure $\langle \partial u_1/\partial x_1 \rangle^2$. The velocity from each wire and their difference was computed digitally from the sampled voltages. In addition to the spatial derivative, the time derivative of the velocity signal was also recorded. The second experiment was done with the probe rotated 90 degrees to measure $\langle \partial u_1/\partial x_1 \rangle^2$.

The triple wire probe shown in Figure 3. was designed to measure all the terms in the dissipation equation assuming locally axisymmetric homogeneous turbulence (George and Hussein 1991). The criteria used in design of this probe were that it have the least amount of probe interference, and acceptable spatial resolution for the derivative measurements. The probe was built from three angle wires. The spacing of the wires was approximately 0.2 mm which is close enough in regards to the Kolomogorov microscale to avoid spatially filtering the derivative signal. This probe was used in two different experiments. In the first, the probe was aligned with the jet in such a way that the terms $\langle \partial u_1/\partial x_1 \rangle^2$, $\langle \partial u_2/\partial x_1 \rangle^2$, $\langle \partial u_2/\partial x_3 \rangle^2$, $\langle \partial u_1/\partial x_3 \rangle^2$, were measured. In the second, the probe was rotated 90 degrees to obtain $\langle \partial u_1/\partial x_1 \rangle^2$, $\langle \partial u_3/\partial x_1 \rangle^2$, $\langle \partial u_3/\partial x_2 \rangle^2$, $\langle \partial u_1/\partial x_2 \rangle^2$.

The hot-wires were calibrated in a low turbulence intensity calibration tunnel. A fourth order polynomial as described in George et al. (1987) was used. The error in predicting the measured velocity from measured voltages was

typically less than 0.1% over the entire range. Once the coefficients were found, they were used for the determination of instantaneous velocity from the instantaneous voltages sampled by the A/D. The calibration data was verified at the end of each experiment to insure that the calibration did not shift during the course of the experiment. The angle calibration for the cross-wires was done using a modified cosine law with a velocity-dependent k-factor (Beuther et al. 1987).

4. Experimental Results

4.1 First and second moments of the velocity field

Figure 4a shows the variation of the centerline mean velocity with the distance from the jet exit. Both the stationary and moving wire results are in excellent agreement with those measured by Capp using LDA and those obtained earlier by Peng (1985) in the same facility using stationary hot-wires. This is, of course, the expected result since the turbulence intensity is a minimum at the centerline and the hot-wire cross-flow errors are less than a few percent of the mean value there. Also shown for comparison is the centerline data of Wygnanski and Fiedler (1969). These have been discussed in detail by Capp (1983) who attributed the difference to problems in their facility (see also Capp et al. 1989, Taulbee et al. 1987).

The data for x/D > 30 are described to within the experimental error by the similarity relationship.

$$\frac{U}{U_o} = \frac{1}{5.9}\left[\frac{X}{D} - 2.7\right] \tag{10}$$

or

$$U = 6.7\sqrt{M_o}\,(x - 2.7D)^{-1} \tag{11}$$

The virtual origin is 2.7 diameters and is consistent with that determined in the Capp (1983) experiment.

The mean axial velocity normalized by the centerline velocity, U/U_c, is plotted versus the non-dimensional radial coordinate, $\eta = r/x$, in Figure 4b. (Note that x is measured from the virtual origin established above.) To avoid clutter, the data of Wygnanski and Fiedler (1969) has been plotted only as a smooth line. The mean profiles of the current facility collapse by 30 diameters with a virtual origin of 2.7 times the diameter of the jet, a value consistent with that obtained from the centerline mean velocity decay. The stationary wire profile gives a half width of 0.102 which is wider that the value of 0.094 obtained with the LDA (Capp 1983). This behavior is expected, since a binomial expansion of

the error in the mean velocity due to cross-flow effects reveals the leading error term is positive. The moving wire results for leading cross-flow error term is less than 5% across the flow.

4.2 The second order moments

The Reynold's stress terms that are non-zero in this axisymmetric jet are $\langle u_1\rangle^2$, $\langle u_2\rangle^2$, $\langle u_3\rangle^2$, $\langle u_1u_2\rangle$. These terms non-dimensionalized by the square of the centerline velocity are shown on Figures 5,6,7 and 8 respectively. The moving wire results for all moments were in very close agreement with the LDA results reported by Capp (1983) (see also Taulbee et al. 1987), but differ substantially from the stationary wire results. This behavior is consistent with the effects of the cross-flow errors which cause greater contamination than for the mean, since for the second-order moments the leading terms are negative and depend on the third order moments.

The inter-consistency of the data and the degree to which the flow represents a free jet can be evaluated by checking to see whether they satisfy the governing equations (v. George 1988). Figures 9,10 and 11 show the measured Reynolds stress for the Stationary wire, LDA and moving wire data. As shown on the figures, the measured Reynolds stress terms are compared to that calculated from the remaining terms in the integrated momentum equation (v. Taulbee et al. 1987). The excellent agreement for the moving wire results (shown on Table II) confirm the validity of the data. The stationary wire data shows a consistent 20% discrepancy across the flow because of the hot wire errors.

4.3 Derivative measurements

The streamwise derivatives of the three velocity components were calculated from their corresponding measured temporal derivatives of $\langle\partial u_1/\partial t\rangle$, $\langle\partial u_2/\partial t\rangle$, $\langle\partial u_3/\partial t\rangle$. The issue of the applicability of Taylor,s hypothesis was addressed by utilizing the flying wire mechanism. Appendix II reproduces analysis for the approximation of Taylor's hypothesis from George et al (1991). The effect of the fluctuating convection velocity is most prominent in the breakdown of Taylor's frozen field hypothesis (Lumley 1965).

To verify the accuracy the frozen field assumption, the mean square derivatives are reported for a rotation rate of one revolution per second and for no rotation at all. The rotation rate chosen corresponds to a ratio of probe velocity to mean centerline velocity of 1.45. Figure 12 shows the radial dependence of the mean square time derivatives for stationary and rotating probes. The contribution of the terms depending on the fluctuating velocity in equation A.II.16 are less than 4% for the rotating probe results, and they therefore are close to the actual values of $\langle\partial u_1/\partial x_1\rangle^2$.

Figure 13 shows the difference between the stationary and moving probe results normalized by the latter and plotted as a function of $[\langle u_1\rangle^2+2*(\langle u_2\rangle^2+\langle u_3\rangle^2)\ ]/\ (U_p+U)^2$. There is clearly a close agreement between the isotropic result of equation A.II.16 and the measured difference as indicated by the line. In summary, the experimental data gives considerable confidence in the theoretical results.

Figure 14 shows the profiles of the velocity derivatives in the streamwise direction. These derivatives satisfy the isotropic relations near the centerline, but progressively deviate from them as the radius increases. On this figure, $\langle \partial u_1/\partial x_1 \rangle^2$, $\langle \partial u_2/\partial x_1 \rangle^2$ and $\langle \partial u_3/\partial x_1 \rangle^2$ measured with the Axi-probe and $\langle \partial u_1/\partial x_1 \rangle^2$ from a different experiment using a parallel wire probe are plotted as a function of radial position across the jet.

The velocity derivatives in the azimuthal direction, $\langle \partial u_1/\partial x_3 \rangle^2$ and $\langle \partial u_2/\partial x_3 \rangle^2$ were measured with the Axi-probe. The correlation term $\langle \partial u_1/\partial x_3 \rangle^2$ was also meausred with the parallel wire probe in a seperate experiment and the reults from both sets of experiments are shown on Figure 15. Another set experiments were performed with the probes rotated by 90°. These experiments were aimed at measuring the velocity derivatives in the radial direction. The results from this experiment, $\langle \partial u_1/\partial x_2 \rangle^2$ and $\langle \partial u_3/\partial x_2 \rangle^2$ measured with the Axi-probe and $\langle \partial u_1/\partial x_2 \rangle^2$ measured with the parallel probe are shown on Figure 16.

Axisymmetry requires that the terms $\langle \partial u_3/\partial x_2 \rangle^2$ be equal to $\langle \partial u_2/\partial x_3 \rangle^2$ and that $\langle \partial u_2/\partial x_1 \rangle^2$ be equal to $\langle \partial u_3/\partial x_1 \rangle^2$. These terms are shown on Figures 15 and 16, and the results shown to within the accuracy of the measurements that the flow appears to be truly axisymmetric in the small scales.

In addition to the above mentioned mean square derivatives, a number of mixed derivative correlations which should be zero in locally axisymmetric or locally isotropic turbulence were also measured. Two sets of these correlations were measured. The first set, $\langle \partial u_1/\partial x_1 \rangle \langle \partial u_2/\partial x_1 \rangle$, $\langle \partial u_1/\partial x_3 \rangle \langle \partial u_2/\partial x_3 \rangle$, $\langle \partial u_2/\partial x_1 \rangle \langle \partial u_1/\partial x_3 \rangle$, $\langle \partial u_2/\partial x_1 \rangle \langle \partial u_2/\partial x_3 \rangle$, $\langle \partial u_2/\partial x_1 \rangle \langle \partial u_2/\partial x_3 \rangle$ and $\langle \partial u_2/\partial x_3 \rangle \langle \partial u_1/\partial x_3 \rangle$ is shown on Figure 17. The other set, $\langle \partial u_1/\partial x_1 \rangle \langle \partial u_3/\partial x_1 \rangle$, $\langle \partial u_1/\partial x_2 \rangle \langle \partial u_3/\partial x_2 \rangle$, $\langle \partial u_3/\partial x_1 \rangle \langle \partial u_1/\partial x_2 \rangle$, $\langle \partial u_3/\partial x_1 \rangle \langle \partial u_3/\partial x_2 \rangle$, $\langle \partial u_3/\partial x_1 \rangle \langle \partial u_3/\partial x_2 \rangle$ and $\langle \partial u_3/\partial x_2 \rangle \langle \partial u_1/\partial x_2 \rangle$ is shown on Figure 18. The corresponding correlation coefficients were less than 5% over most of the jet, verifying that at least these aspects of local axisymmetry or local isotropy were satisfied to within the accuracy of the measurements.

The full implications of this local axisymmetry is presented in George and Hussein (1991). The most significant consequence for the present experiment is that the entire set of derivative correlations can be represented in terms of four invariants which in turn, depend only on measurable quantities. Thus the determination of the dissipation and mean square fluctuating vorticity is limited only by the measurement accuracy of the four independent derivatives.

4.4 Dissipation

Figure 19 shows the comparison between ϵ_{axs} obtained with the assumption of local axisymmetry and ϵ_{iso}, calculated from $\langle \partial u_1/\partial x_1 \rangle^2$ and $\langle \partial u_1/\partial x_2 \rangle^2$ assuming local isotropy. For the jet, the isotropic results differ from the dissipation by about 25% at the centerline and by about 40% near the point of maximum mean shear ($r/x = 0.1$). The results show no evidence of the off-axis peak reported by Taulbee et al. (1987) who calculated the dissipation as a closing term in the energy balance. In view of the present data, the off-axis peak in their calculation can probably be attributed to inaccuracies in the determination of the derivatives of the measured second and third moments near the axis.

5. Summary and Conclusions

The velocity field and the statistical correlations of a number of the mean square derivatives in the dissipation tensor are presented for the axisymmetric turbulent jet. Three of the mean square derivatives were computed from their corresponding measured temporal derivatives. The use of the moving wire probe which reduces the effective turbulence intensity provides the only way to measure these terms accurately in this flow, since Taylor's frozen field hypothesis does not accurately apply to the stationary wire results. Having obtained a set of data with and without moving the wire, an assessment of the breakdown of this hypothesis was done. It was found that the correction model which was introduced by Lumley (1965) and George (1979) for the effect of the fluctuating convection velocity on temporal derivatives measured with stationary probes gives good results.

The issue of cross-flow and rectification errors was addressed with pertinence to the use of hot wires in flows with turbulence intensities that is higher than 30%. Comparisons between the results of the moving wire and stationary wire enabled the evaluation of these errors. The results of the error analysis for the moments of the velocity field were presented in this work.

This work also provides a considerable amount of data on the dissipative scales of turbulence for the isothermal axisymmetric jet. It was proven that the jet is not locally isotropic but rather locally axisymmetric in the small scale. The direct measurement of the dissipation is presented for the first time for this type of flow.

ACKNOWLEDGEMENTS

This work was carried out primarily at the Turbulence Research Laboratory at Buffalo, SUNY, and formed a portion of the Ph.D. dissertation of HJH. Earlier versions of this work were presented by the authors at the 1988 and 1989 Annual Meetings of the American Physical Society, Division of Fluid Mechanics.

This research was supported by the National Science Foundation Fluid Mechanics Program under Grant Number MSM 8316833.

REFERENCES

Batchelor, G.K. (1946) "Theory of Axisymmetric Turbulence", Proc. Roy. Soc. A, 186, 480.

Beuther, P.D., A. Shabbir and W.K. George (1987) "X-Wire Response in Turbulent Flows with High Intensity Turbulence and Low Mean Velocity", ASME Proc. Symp. on Thermal Anemometry, Cincinnati, OH.

Cantwell, B. and C. Coles (1983) "An Experimental Study of Entrainment and Transport in the Turbulent Near Wake of a Circular Cylinder, J. Fluid Mech. 136, 321-374.

Capp, S.P., Hussein, H.J., and W.K. George (1989) "Turbulence Measurements in a Momentum Conserving Axisymmetric Jet," Turbulence Research Laboratory Dept. 123, SUNY/Buffalo.

Capp, S.P. (1983) "Experimental Investigation of the Turbulent Axisymmetric Jet", PhD Dissertation, University at Buffalo, SUNY.

Champagne, F.H. (1978) "The Fine Scale Structure of the Turbulent Velocity Field", J. Fluid Mech., 86, Pt. 1, 67.

Chandrasekhar, S. (1950) "Theory of Axisymmetric Turbulence", Proc. Roy Soc. A., 242, 855.

Doughman, E.L. (1972) "Development of a Hot-Wire Anemometer for Hypersonic Turbulent Flows", The Review of Scientific Instruments, 43, 8, 1200.

George, W.K. and P.D. Beuther (1979) "Interpretation of Turbulent Measurements in High Intensity Shear Flow", Bull. Am.Phys.Soc., Ser.II, 24, No.8.

George, W.K., Capp, S.P., Seif, A.A., Baker, C.B. and D.B. Taulbee "A Study of the Turbulent Axisymmetric Jet", J. Engr. Sci., 14, 1, 85-93.

George, W.K. and H.J. Hussein (1991) "Locally Axisymmetric Turbulence", to appear in Journal of Fluid Mechanics, 1991.

George, W.K., P.D. Beuther and A. Shabbir (1987) "Polynomial Calibrations for Hot Wires in Thermally Varying Flows", ASME Appl. Mech., Bioengr and Fluids Engr. Conf., Cincinnati, OH.

George, W.K. (1988) "Governing Equations, Experiments and the Experimentalist", 1st World Conference on Heat Transfer, Fluid Mechanics and Thermodynamics, Dubrovnik, Yugoslavia, Sept. 5-9.

Hussein, H.J., (1988) "Measurements of small scale turbulence in an axisymmetric jet using moving hot wires", PhD Dissertation, University at Buffalo, SUNY.

Lumley, J.L. (1965) "Interpretation of Time Spectra Measured in High-Intensity Shear Flows" Physics of Fluids, 8, 1056-1062.

Lumley (1978), "Computational modeling of Turbulent Flows", Advances in Applied Mechanics, 18, 123-176.

Panchapakesan, N.R. and J.L. Lumley (1986) "Round Jet Measurements with a Hot-Wire Probe Mounted on a Shuttle", Bull. Am.Phys. Soc., Ser. II, 31, #10.

Peng, D. (1985) "Hot-Wire Measurements in a Momentum Conserving Axisymmetric Jet", MS Thesis, University at Buffalo, SUNY.

Taulbee, D.B., H.J. Hussein and S.P. Capp (1987) "The Round Jet Experiment and Inferences on Turbulence Modeling", 6th Symp. on Turbulent Shear Flows, Toulouse, France.

Tutu, N. and R. Chevray (1975) "Cross-wire Anemometry in High Intensity Turbulence" J. Fluid Mechanics, 71, 785-800.

Uberoi, M.S. (1975) Presentation at APS/DFD 36th Annual Meeting, College Park, MD. 20.

Watmuff, J.H., A.E. Perry and M.S. Chang (1983) "A Flying Hot-Wire System", Experiments in Fluids, 1, 63-71.

Wyngaard, J.C. (1968) "Measurement of Small Scale Turbulence Structure with Hot-Wires", J. Sc. Instrum. 1, 1105-1108.

Wygnanski, I. and H.E. Fiedler (1969) "Some Measurements in the Self Preserving Jet" J. Fluid Mechanics, 38, 577-612.

LIST OF TABLES

TABLE I

JET EXIT CONDITIONS

QUANTITY	SYMBOL	VALUE
Exit Diameter (m)	D	.0255
Velocity (m/s)	U_o	55.0
Volume Rate (m^3/s)	m_o	0.277
Momentum Rate/Unit Mass (m^4/s^2)	M_o	1.51
Reynolds Number	Re_o	9.2×10^4

TABLE II

MOMENTUM INTEGRAL RESULTS

	U^2	$\langle u_1 \rangle^2$	$\langle u_2 \rangle^2$	$\langle u_3 \rangle^2$	Total
LDA	0.87	0.24	0.13	0.15	0.97
HW	0.99	0.14	0.07	0.05	1.07
FHW	0.914	0.193	0.044	0.058	1.005

TABLE III. Curve Fits For Even Functions.

Value	Probe Type	C_0	C_2	C_4	C_6	D	Error
U	L HW FHW	1.0 1.0 1.0	1.212E-1 -1.925 -4.84	2.185 E3 -- 1.27 E3		111 63 84	2.60E-3
$\overline{u^2}$	L HW FHW	7.648E-2 7.779E-2 7.73 E-2	1.729E-1 2.79 E-1 1.459E-1	-4.845 E2 -2.02 E3 1.11 E2	5.864E4 4.30 E5 1.4 E4	156 257 147	2.49 E-4
$\overline{v^2}$	L HW FHW	4.723E-2 5.457E-2 5.14 E-2	2.222 0.355 3.32	5.174E-1 -42.98 1.484E-1		79 89 120	4.52E-5
$\overline{w^2}$	L HW FHW	4.900E-2 5.78 E-2 5.26 E-2	2.316 -1.71 3.22	5.754E-1 2.173E-1 3.49 E+2		73 42 133	5.20E-5
$\overline{u^3}$	L HW FHW	2.139E-3 2.14 E-3	2.348 1.008	-1.551 -4.763E+1	1.889E3 5.54 E2	134 75	
$\overline{uv^2}$	L HW FHW	-1.25E-3 2.200E-3	8.746E-1 1.237	-7.080E-1 -5.288E+1	8.995E2 7.81 E2	135 95	
$\overline{uw^2}$	L HW FHW	-1.246E3 2.25 E-3	6.665E-1 1.04 E-1	-7.729 -9.20 E+2	1.133E3 1.98 E4	155 65	

Table IV Curve Fits For Odd Functions.

Value	Probe Type	C_1	C_3	C_5	C_7	D
$\overline{uv}$	L HW FHW	5.500E-1 4.375E-1 4.89 E-1	-2.96E-1 -3.93E-1 -6.451	1.282 E3 1.55 E2 4.095 E3	-1.898E4 1.342 E4 -1.057E5	78 90 147
$\overline{vu^2}$	L HW FHW	3.870E-2 3.33 E-2	2.647E-1 1.59 E-1	-7.988E2 -2.87 E2	5.340 E4	196 169
$\overline{v^3}$	L HW FHW	4.870E-2 1.2 E-1	3.518E-1 7.29 E-1	6.771 2.09 E3	-6.250E2	65 246.00
$\overline{vw^2}$	L HW FHW	-- 3.0 E-2 --	-- 5.17 --	-- -4.83 E2	-- 7.527 E3	 100.0

Appendix I Locally-axisymmetric homogeneous turbulence

It have been of considerable interest to turbulence modelers and theoreticians to obtain measurements of the rate of dissipation of turbulence kinetic energy, ϵ , given by (Hinze 1975):

$$\epsilon = 2\nu\left\{\left[\left\langle\frac{\partial u_1}{\partial x_1}\right\rangle^2 + \left\langle\frac{\partial u_2}{\partial x_2}\right\rangle^2 + \left\langle\frac{\partial u_1}{\partial x_3}\right\rangle^2\right]\right.$$

$$+ \frac{1}{2}\left[\left\langle\frac{\partial u_1}{\partial x_2}\right\rangle^2 + \left\langle\frac{\partial u_1}{\partial x_3}\right\rangle^2 + \left\langle\frac{\partial u_2}{\partial x_1}\right\rangle^2\right. \qquad \text{AI.1}$$

$$\left.+\left\langle\frac{\partial u_2}{\partial x_3}\right\rangle^2 + \left\langle\frac{\partial u_3}{\partial x_1}\right\rangle^2 + \left\langle\frac{\partial u_3}{\partial x_2}\right\rangle^2\right] + \left[\left\langle\frac{\partial u_2}{\partial x_1}\right\rangle\left\langle\frac{\partial u_1}{\partial x_2}\right\rangle\right.$$

$$\left.\left.+\left\langle\frac{\partial u_3}{\partial x_1}\right\rangle\left\langle\frac{\partial u_1}{\partial x_3}\right\rangle + \left\langle\frac{\partial u_3}{\partial x_2}\right\rangle\left\langle\frac{\partial u_2}{\partial x_3}\right\rangle\right]\right\}$$

The direction measurement of the average dissipation and mean square vorticity clearly requires measurements of various components of the spatial derivatives. Because of the near impossibility of this in practice, investigators have usually relied on the assumption of local isotropy and Taylor's frozen field hypothesis in determining the dissipation.

For isotropic turbulence (Hinze 1975):

$$2\left\langle\frac{\partial u_1}{\partial x_1}\right\rangle^2 = \left\langle\frac{\partial u_1}{\partial x_2}\right\rangle^2 = \left\langle\frac{\partial u_1}{\partial x_3}\right\rangle^2 = \left\langle\frac{\partial u_2}{\partial x_1}\right\rangle^2 = \left\langle\frac{\partial u_2}{\partial x_3}\right\rangle^2 = \left\langle\frac{\partial u_3}{\partial x_1}\right\rangle^2 = \left\langle\frac{\partial u_3}{\partial x_2}\right\rangle^2 \qquad \text{AI.2}$$

$$\left\langle\frac{\partial u_1}{\partial x_1}\right\rangle^2 = \left\langle\frac{\partial u_2}{\partial x_2}\right\rangle^2 = \left\langle\frac{\partial u_3}{\partial x_3}\right\rangle^2 \qquad \text{AI.3}$$

$$\left\langle \frac{\partial u_1}{\partial x_2} \right\rangle \left\langle \frac{\partial u_2}{\partial x_1} \right\rangle = \left\langle \frac{\partial u_1}{\partial x_3} \right\rangle \left\langle \frac{\partial u_3}{\partial x_1} \right\rangle = \left\langle \frac{\partial u_2}{\partial x_3} \right\rangle \left\langle \frac{\partial u_3}{\partial x_2} \right\rangle = -\frac{1}{2} \left\langle \frac{\partial u_1}{\partial x_1} \right\rangle^2 \qquad \text{AI.4}$$

Thus only measurement of $\langle \partial u_1/\partial x_1 \rangle^2$ is necessary. This has been usually accomplished by measuring only the temporal derivative of the longitudinal components of the velocity and using Taylor's frozen field hypothesis.

The assumption of local isotropy simplified the experiments significantly but the accuracy of the results were impaired by the fact that shear flows such as the jet did not usually satisfy the relations for local isotropy. For the jet, this anisotropy of the small scales becomes more pronounced the farther one gets form the centerline.

From the measurement of seven of the terms in equation (3) it was clear from the data that these derivative measurements did not satisfy the conditions for local isotropy. However, they were found to satisfy the conditions for axisymmetric homogeneous turbulence (Batchelor 1946, Chandrasekar 1950) to within the experimental error. Thus it is appropriate to use the concept of locally axisymmetric turbulence introduced by George and Hussein (1991) for which

$$\left\langle \frac{\partial u_1}{\partial x_2} \right\rangle^2 = \left\langle \frac{\partial u_1}{\partial x_3} \right\rangle^2 \qquad \text{AI.5}$$

$$\left\langle \frac{\partial u_2}{\partial x_1} \right\rangle^2 = \left\langle \frac{\partial u_3}{\partial x_1} \right\rangle^2 \qquad \text{AI.6}$$

$$\left\langle \frac{\partial u_2}{\partial x_2} \right\rangle^2 = \left\langle \frac{\partial u_3}{\partial x_3} \right\rangle^2 \qquad \text{AI.7}$$

$$\left\langle \frac{\partial u_2}{\partial x_3} \right\rangle^2 = \left\langle \frac{\partial u_3}{\partial x_2} \right\rangle^2 \qquad \text{AI.8}$$

$$\left\langle \frac{\partial u_2}{\partial x_2} \right\rangle^2 = \frac{1}{3} \left\langle \frac{\partial u_1}{\partial x_1} \right\rangle^2 + \frac{1}{3} \left\langle \frac{\partial u_2}{\partial x_3} \right\rangle^2 \qquad \text{AI.9}$$

$$\left\langle \frac{\partial u_1}{\partial x_2} \right\rangle \left\langle \frac{\partial u_2}{\partial x_1} \right\rangle = \left\langle \frac{\partial u_1}{\partial x_3} \right\rangle \left\langle \frac{\partial u_3}{\partial x_1} \right\rangle = -\frac{1}{2} \left\langle \frac{\partial u_1}{\partial x_1} \right\rangle^2 \qquad \text{AI.10}$$

$$\left\langle \frac{\partial u_2}{\partial x_3} \right\rangle \left\langle \frac{\partial u_3}{\partial x_2} \right\rangle = \frac{1}{6} \left\langle \frac{\partial u_1}{\partial x_1} \right\rangle^2 - \frac{1}{3} \left\langle \frac{\partial u_2}{\partial x_3} \right\rangle^2 \qquad \text{AI.11}$$

From equation (3) it follows immediately that

$$\epsilon = \nu \left[\frac{5}{3} \left\langle \frac{\partial u_1}{\partial x_1} \right\rangle^2 + 2 \left\langle \frac{\partial u_1}{\partial x_2} \right\rangle^2 + 2 \left\langle \frac{\partial u_2}{\partial x_1} \right\rangle^2 + \frac{8}{3} \left\langle \frac{\partial u_2}{\partial x_3} \right\rangle^2 \right] \qquad \text{AI.1}$$

For isotropic turbulence equation (12) reduces to the familiar result,

$$\epsilon = 15\nu \left\langle \frac{\partial u_1}{\partial x_1} \right\rangle^2 \qquad \text{AI.13}$$

Appendix II - The Application of Taylor's Hypothesis to Velocity Derivative Measurements.

Lumley (1965) and Wyngaard and Clifford (1977) have presented analyses of the effect of the fluctuating correction velocity on the Spectral and derivative analyses. In both cases, the analysis of the fluctuating derivatives began with the truncation of an assumed Gaussian Characteristic function for the turbulence, and it was therefore believed to be limited in some manner. The purpose of the brief analysis below which is due to George and Beuther (1979), is to illustrate that their result can be obtained without the Gaussian assumption, and should therefore be applicable over a wider range of turbulence intensities than might have been believed from the earlier analysis.

We begin by analyzing the response of a randomly moving probe in a homogeneous velocity field u (x). Let us assume the probe to respond only to the 1 - component of the turbulent velocity. Let us further assume that the turbulent field is frozen and that the probe moves through it. The time varying signal seen by the probe moves through it. The time varying signal seen by the probe can be written as:

$$u_m(t) = \int e^{ik \cdot x_p} \hat{u}(k)\, dk \qquad \text{A.II.1}$$

Where $\underline{x}^p$ (t) represents the motion of the probe and $\hat{u}$ is the Fourier transform of the velocity field.

We seek a relation between the time derivative of $u_m(t)$ and the spatial derivative of $u(\underline{x})$.

Differentiating equation (1) we have,

$$\dot{u}_m = \int e^{ik \cdot x_p} \, (ik \cdot \dot{x}_p) \, \hat{u}(k)\, dk \qquad \text{A.II.2}$$

From which it follows that

$$\overline{(\dot{u}_m)^2} = -\iint e^{i(k-k') \cdot x_p} \, (k \cdot \dot{x}_p) \, (k' \cdot \dot{x}_p) \, \hat{u}(k) \, \hat{u}^*(k') \, dk \, dk' \qquad \text{A.II.3}$$

If we assume the motion of the probe to be statistically independent from the turbulence we can write

$$\overline{(\dot{u}_m)^2} = -\int e^{i(k-k') \cdot x_p} \, (k \cdot \dot{x}_p) \, (k' \cdot \dot{x}'_p) \, u(\hat{k}) \, u(\hat{k}') \, dk dk' \qquad \text{A.II.4}$$

Since the field is assume homogeneous

$$\hat{u}(k) \, \hat{u}^*(k') \, dk \, dk' = F_{11}(k) \, \delta(k' - k) \, dk \, dk'' \qquad \text{A.II.5}$$

Where F_{11} is the three dimensional spectrum of the turbulent velocity.

The position of the probe is simply the time integral of its velocity added to its initial position, i. e.

$$x_p(t) = x_p\,(0)\; t \int_0^t \underline{\tilde{u}}_p\,(t_1)\; dt_1 \qquad \text{A.II.6}$$

Where $\underline{\tilde{u}}_p$ is the instantaneous probe velocity. Thus

$$\dot{x}_p(t) = \tilde{u}_p(t) = \underline{U}_p + \underline{u}_p \qquad \text{A.II.7}$$

Where $\underline{U}_p$ is the mean probe velocity and $\underline{u}_p$ is it's fluctuating component. It follows immediately that

$$\overline{[\dot{u}_m(t)]^2} = \int \overline{[\underline{k}\cdot\underline{U} + \underline{k}\cdot\underline{u}_p]^2}\; F_{11}\;(\underline{k})\; d\underline{k} \qquad \text{A.II.8}$$

We consider the mean motion of the probe to be only in the 1 - direction while we allow its fluctuating motion to be in all directions, i.e.,

$$\underline{U}_p(U_p,\ 0,\ 0) \qquad \text{A.II.9}$$

and $\underline{u}_p = (u_{p_1},\ u_{p_2},\ u_{p_3})$

Inserting these into equation (7) yields the measures mean square time derivative as

$$\begin{aligned}
\overline{[\dot{u}_m(t)]^2} = {} & U_p^2 \int k_1^2\; F_{11}\;(\underline{k})\; d\underline{k} \\
& + \overline{u_{p_1}^2} \int k_1^2\; F_{11}\;(\underline{k})\; d\underline{k} \\
& + 2\,\overline{u_{p_1} u_{p_2}} \int k_1\, k_2\; F_{11}\;(\underline{k})\; d\underline{k} \\
& + 2\,\overline{u_{p_1} u_{p_3}} \int k_1\, k_3\; F_{11}\;(\underline{k})\; d\underline{k} \\
& + \overline{u_{p_2}^2} \int k_2^2\; F_{11}\;(\underline{k})\; d\underline{k} \\
& + 2\,\overline{u_{p_2} u_{p_3}} \int k_2\, k_3\; F_{11}\;(\underline{k})\; d\underline{k} \\
& + \overline{u_{p_3}^2} \int k_3^2\; F_{11}\;(\underline{k})\, d\underline{k}
\end{aligned} \qquad \text{A.II.10}$$

The integral of equation (8) can be readily recognized as the mean square velocity derivatives.

Thus

$$\overline{(u_m)^2} = \overline{(U_{p_1} + u_{p_1})^2} \overline{\left(\frac{\partial u_1}{\partial x_1}\right)^2} + \overline{(u_{p_2}^2)} \overline{\left(\frac{\partial u_1}{\partial x_2}\right)^2}$$

$$+ \overline{(u_{p_3})^2} \overline{\left(\frac{\partial u_1}{\partial x_3}\right)^2}$$

$$+2 \overline{u_{p_1} u_{p_2}} \overline{\left[\frac{\partial u_1}{\partial x_1} \frac{\partial u_1}{\partial x_2}\right]} \qquad \text{A.II.11}$$

$$+ 2 \overline{u_{p_1} u_{p_3}} \overline{\left[\frac{\partial u_1}{\partial x_1} \frac{\partial u_1}{\partial x_3}\right]}$$

$$+2 \overline{u_{p_2} u_{p_3}} \overline{\left[\frac{\partial u_1}{\partial x_2} \frac{\partial u_1}{\partial x_3}\right]}$$

$$+2 \overline{u_{p_2} u_{p_3}} \overline{\left[\frac{\partial u_1}{\partial x_2} \frac{\partial u_1}{\partial x_3}\right]}$$

For homogeneous flow

$$\overline{\left[\frac{\partial u_1}{\partial x_1} \frac{\partial u_1}{\partial x_2}\right]} = \overline{\left[\frac{\partial u_1}{\partial x_1} \frac{\partial u_1}{\partial x_3}\right]} = \overline{\left[\frac{\partial u_1}{\partial x_2} \frac{\partial u_1}{\partial x_3}\right]} = 0 \qquad \text{A.II.12}$$

Therefore;

$$\overline{\left[u_m^2\right]}^2 = U_{p_1}^2 \overline{\left[\frac{\partial u_1}{\partial x_1}\right]}^2 + \overline{u_{p_1}}^2 \overline{\left[\frac{\partial u_1}{\partial x_1}\right]}^2 + \overline{u_{p_2}}^2 \overline{\left[\frac{\partial u_1}{\partial x_2}\right]}^2 + \overline{u_{p_3}}^2 \overline{\left[\frac{\partial u_1}{\partial x_3}\right]}^2 \qquad \text{A.II.13}$$

At this point we identify our probe velocity to be equal and opposite to the Local Fluid Velocity (which corresponds to a probe at rest in a moving field). In doing this, we of necessity violate the condition of independence of probe and fluid motions introduced earlier. However, we may assume the condition to be approximately valid if we confine our attention to the small scale turbulence which is nearly independent of that containing the turbulent energy (Lumley (1965)) has discussed time validity of this). The assumption is particularly good if we confine our attention to high turbulence Reynolds Number Flows because we are interested only in mean square velocity gradients which receive their primary contribution from the dissipative scales, while the convection of disturbances past the probe is primarily due to the move energetic turbulence.

If we are further willing to assume the small scale turbulence to be locally isotropic, the derivatives are related by

$$\overline{\left(\frac{\partial u_1}{\partial x_2}\right)^2} = \overline{\left(\frac{\partial u_1}{\partial x_3}\right)^2} = 2\overline{\left(\frac{\partial u_1}{\partial x_1}\right)^2} \qquad \text{A.II.14}$$

Using these, the mean square derivative signal seen by a stationary probe in a moving turbulent field is,

$$\frac{\overline{u_m^2}}{U^2} = \overline{\left(\frac{\partial u_1}{\partial x_1}\right)^2}\left[1 + \frac{\overline{u_1^2}}{U^2} + 2\frac{\overline{u_2^2} + \overline{u_3^2}}{U^2}\right] \qquad \text{A.II.15}$$

Thus the primitive application of Taylor's hypothesis to the time derivative of the streamwise velocity yields a value of $\overline{\left(\frac{\partial u_1}{\partial x_1}\right)^2}$ which is too high by a factor of

$$\frac{\overline{\left(\frac{\partial u_1}{\partial x_1}\right)^2}}{\overline{\left(\frac{\partial u_1}{\partial u_1}\right)^2}} m = \left[1 + \frac{\overline{u_1^2}}{U^2} + 2\left(\frac{\overline{u_2^2} + \overline{u_3^2}}{U^2}\right)\right] \qquad \text{A.II.16}$$

LIST OF FIGURES

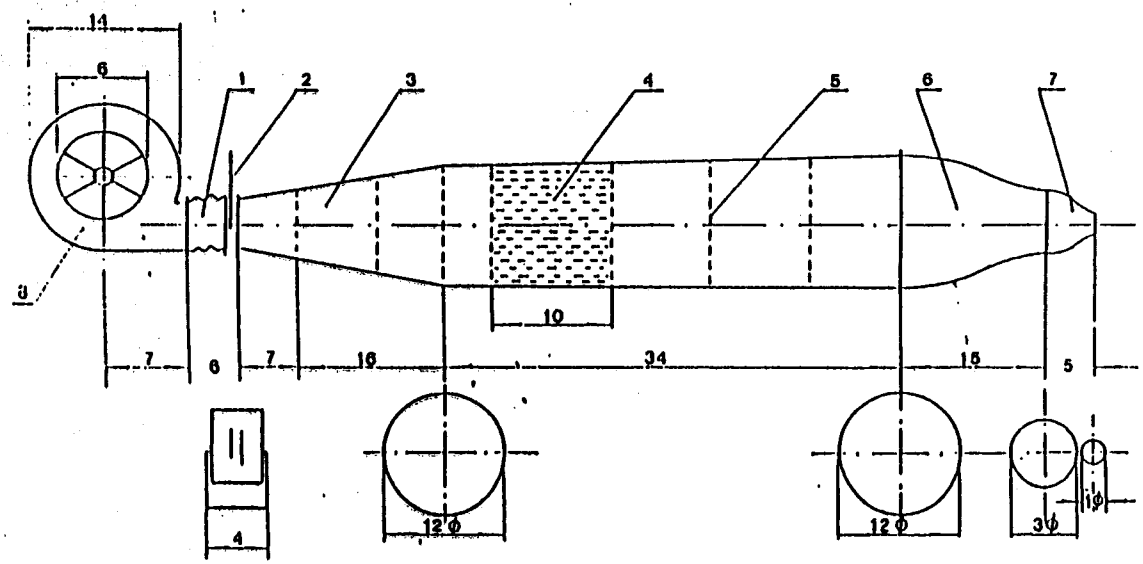

JET FACILITY (ALL DIMENSIONS IN INCHES)

1. VIBRATION ISOLATION	4. HONEY COMB	7. JET
2. SLOT AND PLATE	5. SCREEN	8. BLOWER
3. DIFFUSER	6. NOZZLE	

Figure 1. Sketch of Jet

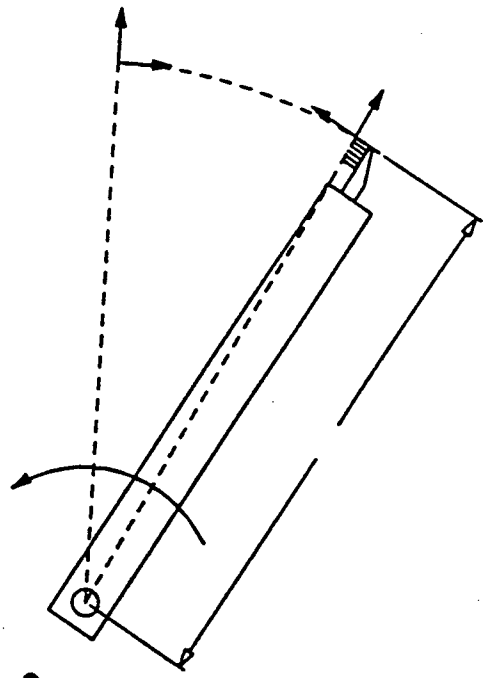

Figure 2. Sketch of moving probe apparatus.

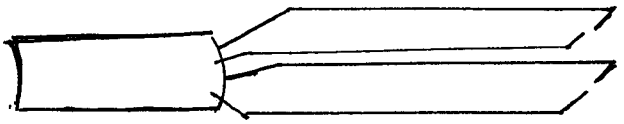

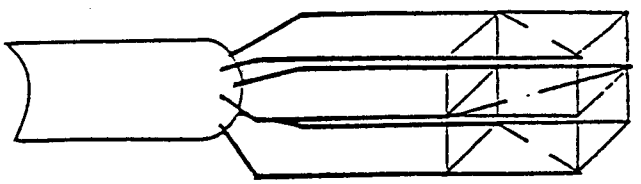

Figure 3

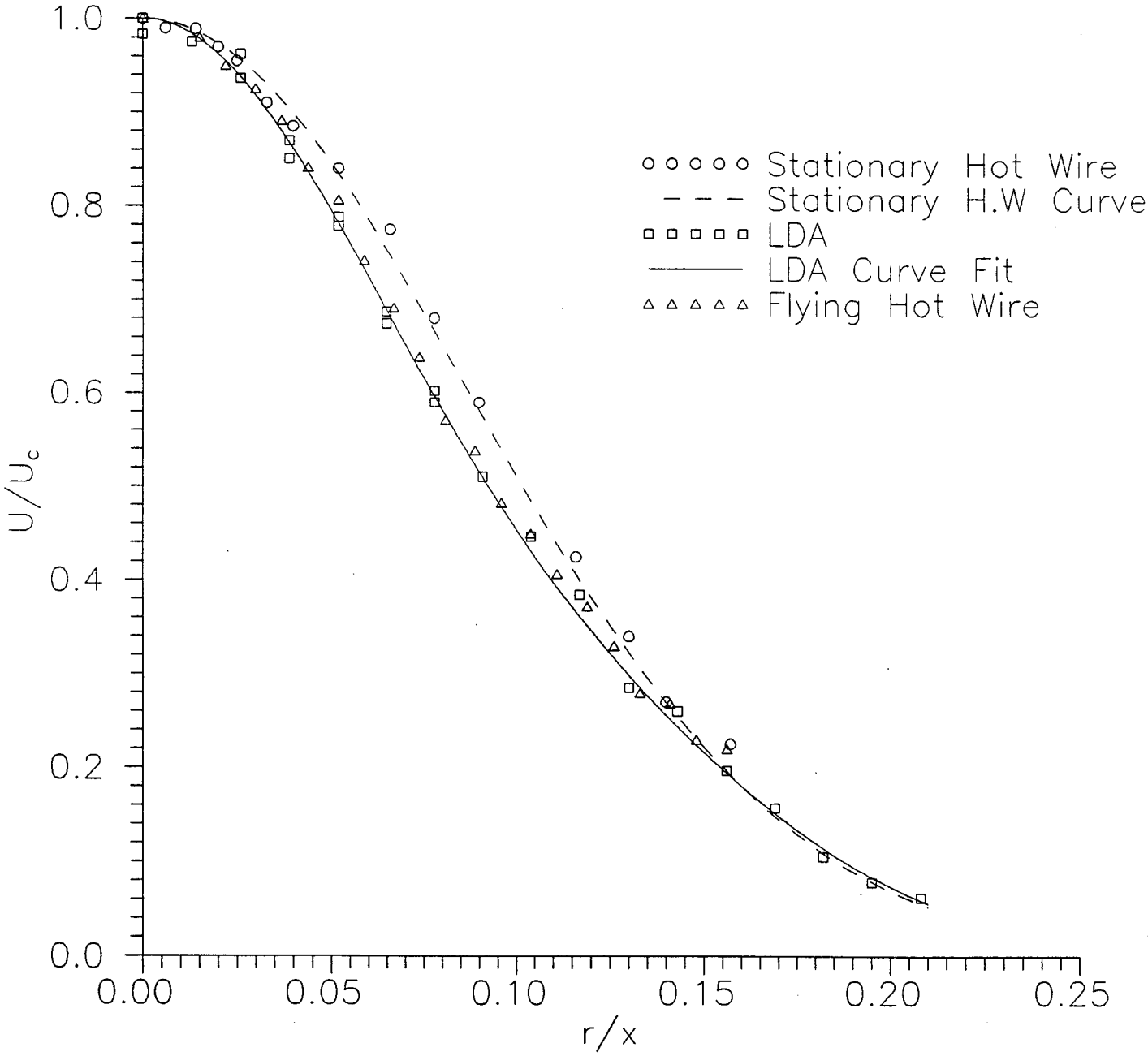

Figure 4**b.** Mean velocity profile

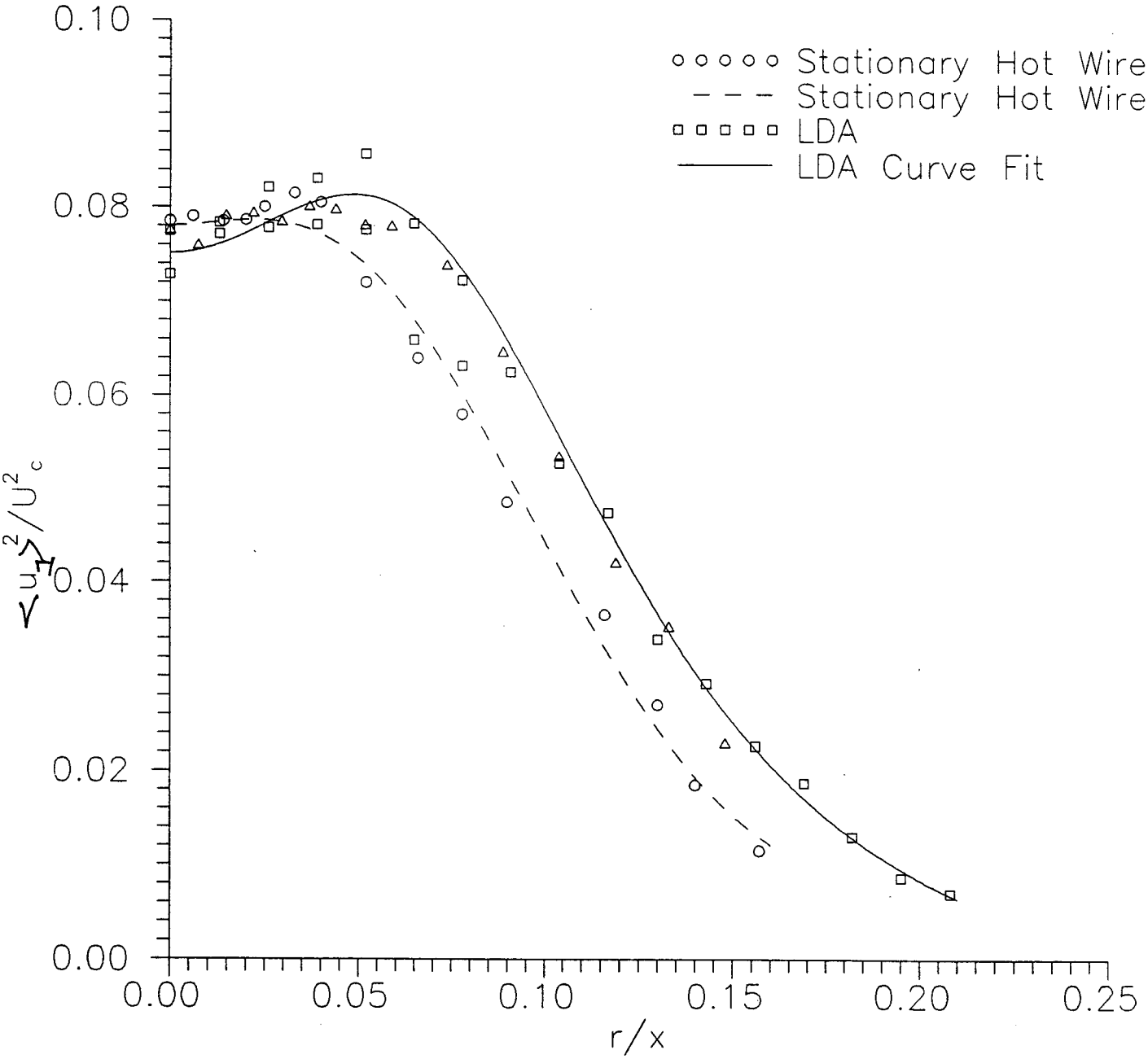

Figure 5. Axial Component, Turbulent Kinetic Energy u_1^2/U_c^2

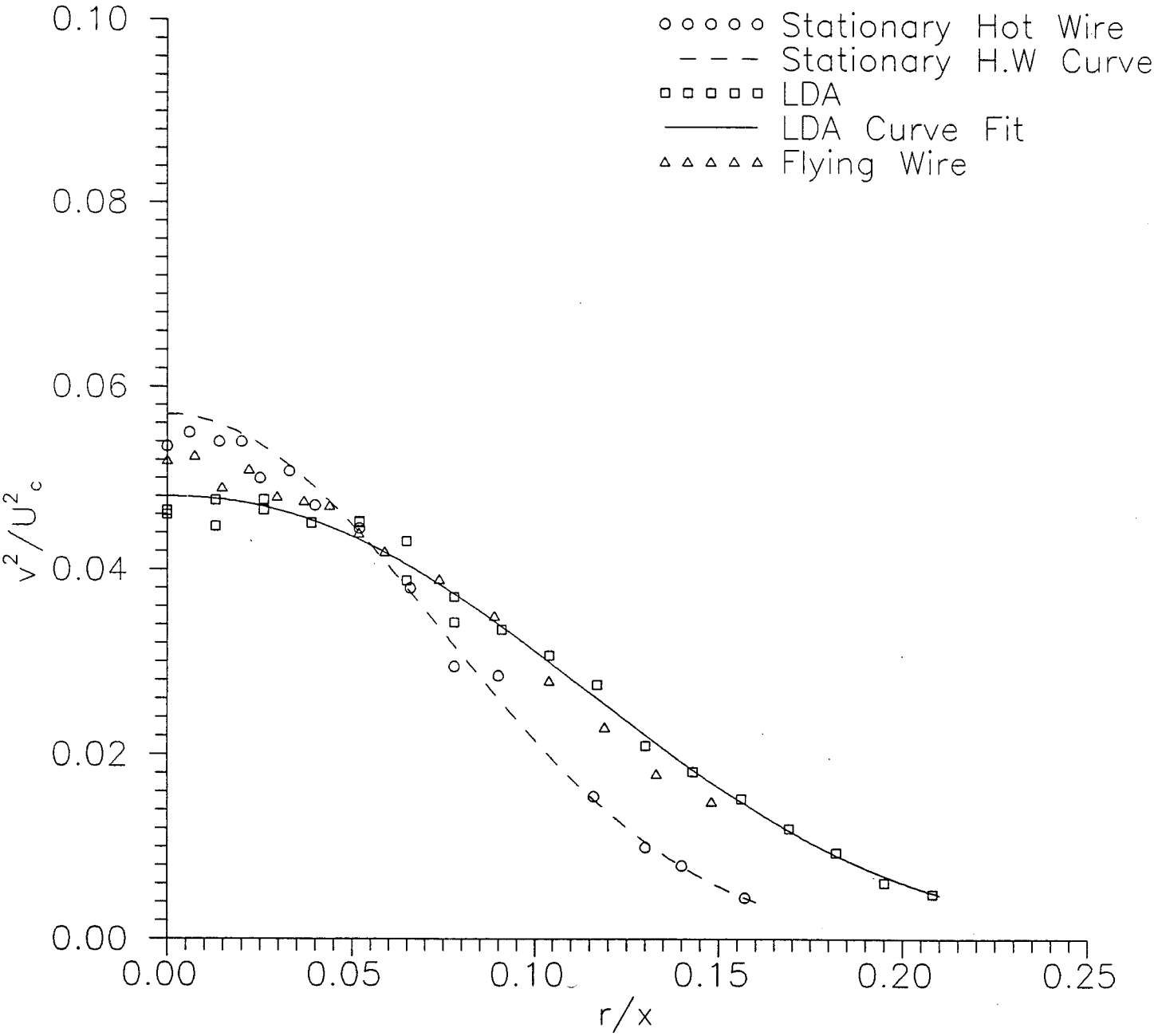

Figure 6. Radial Component, Turbulent Kinetic Energy, v^2/U^2_c

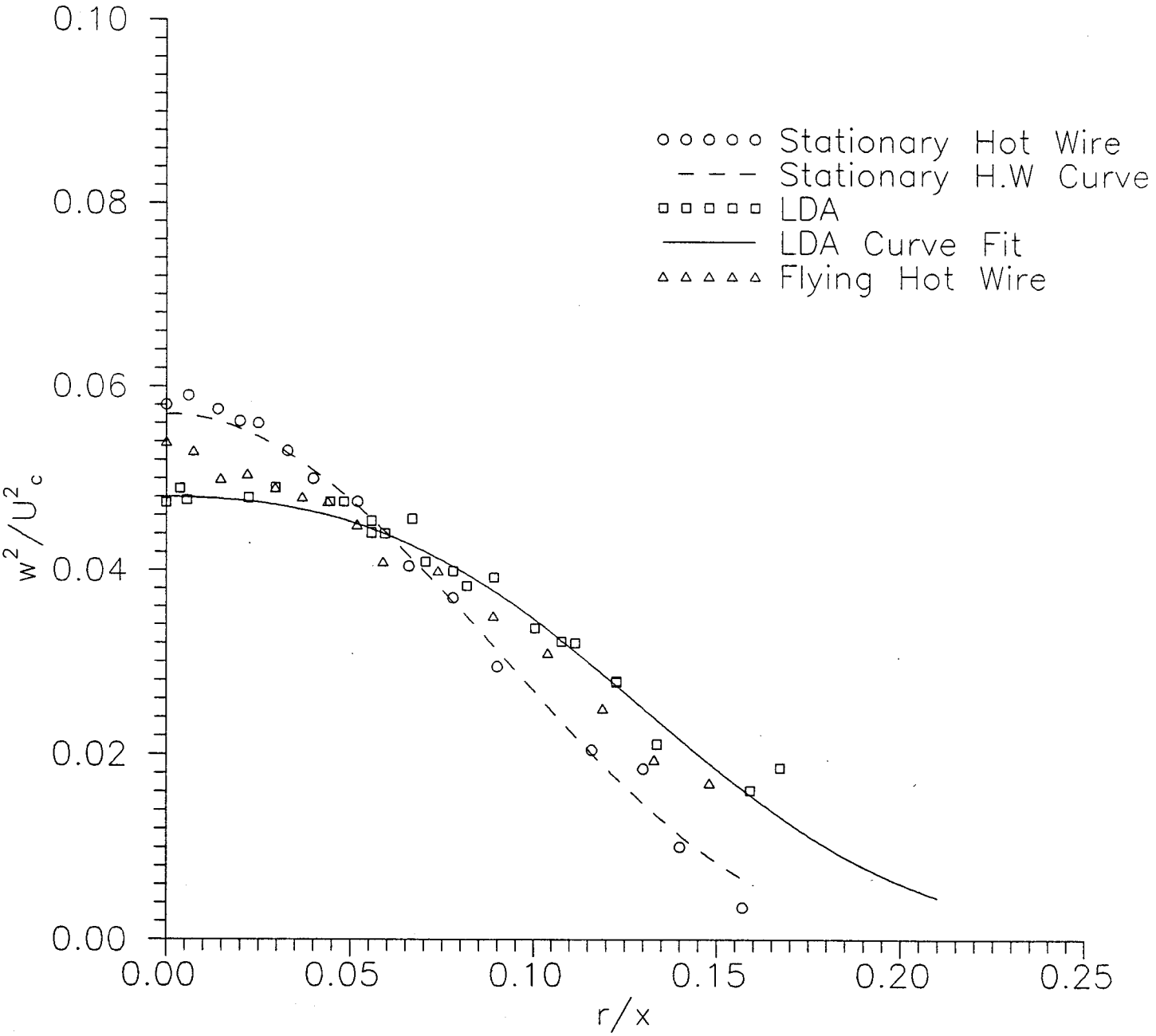

Fiigure. 7 Azimuthal Component, Turbulent Kinetic energy, $\overline{w^2}/U^2_c$

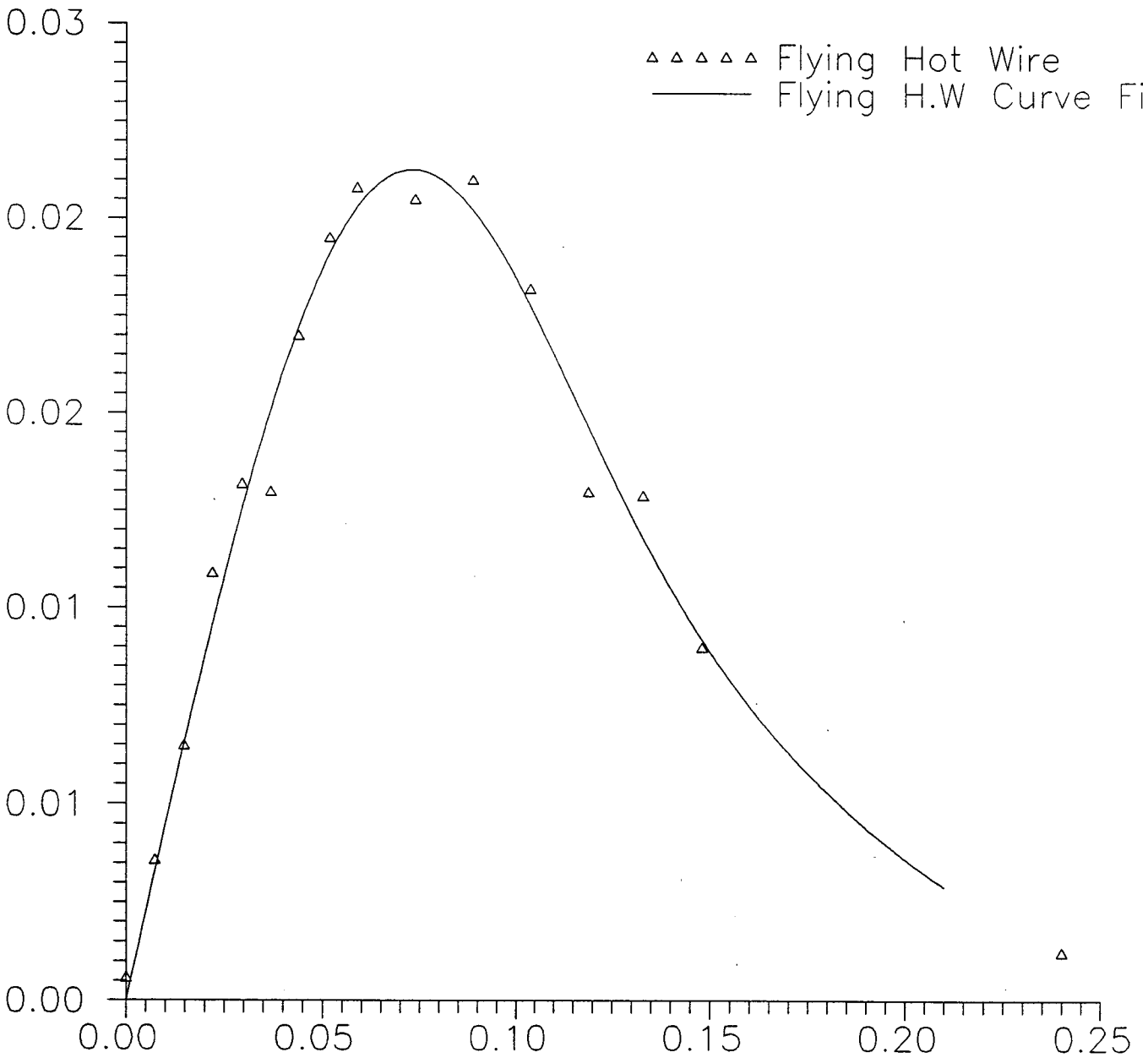

Figure. 8 Shear Stress u_1u_2/U^2_c

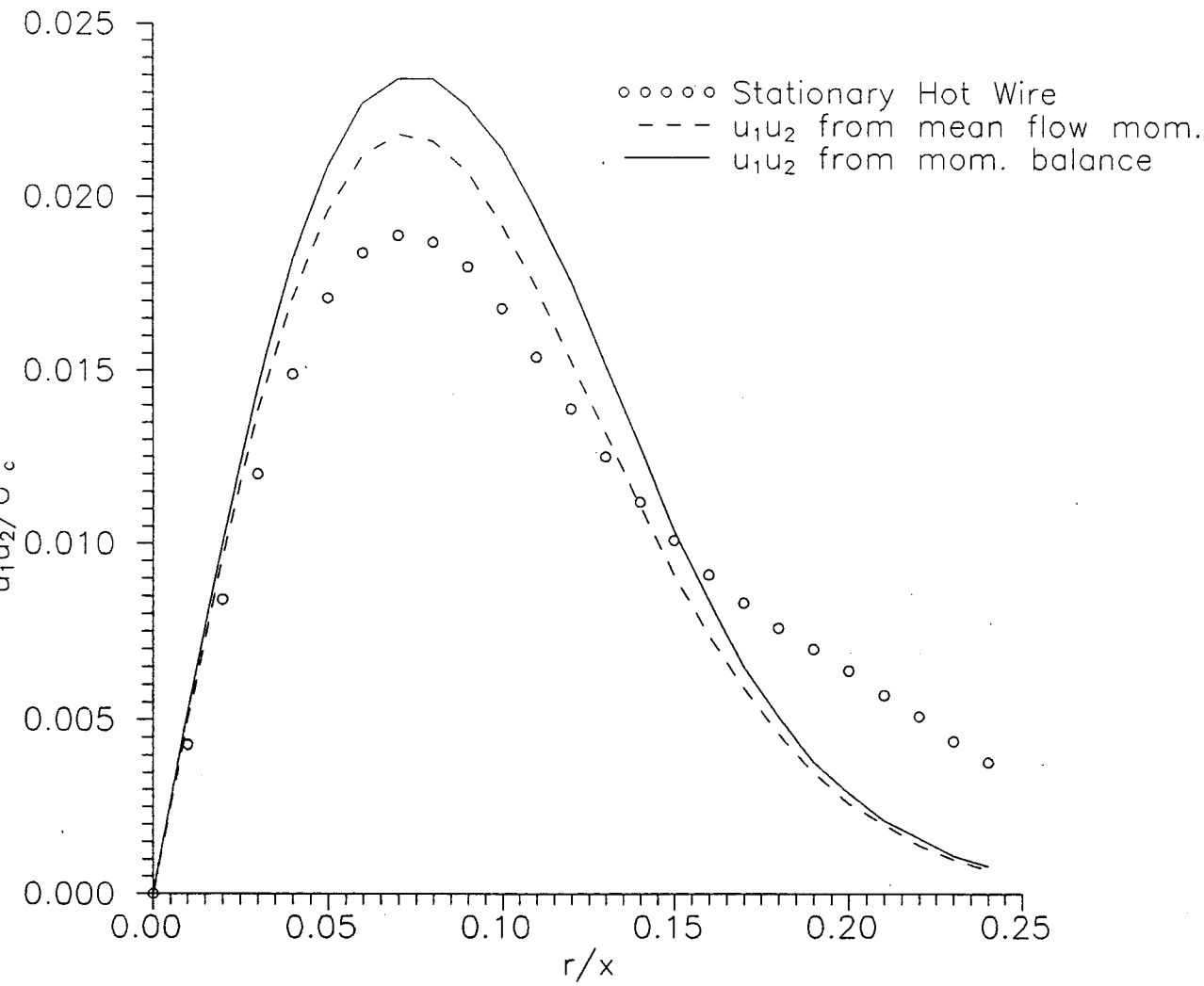

Figure. 9 Turbulent Shear Stress, u_1u_2/U^2_c

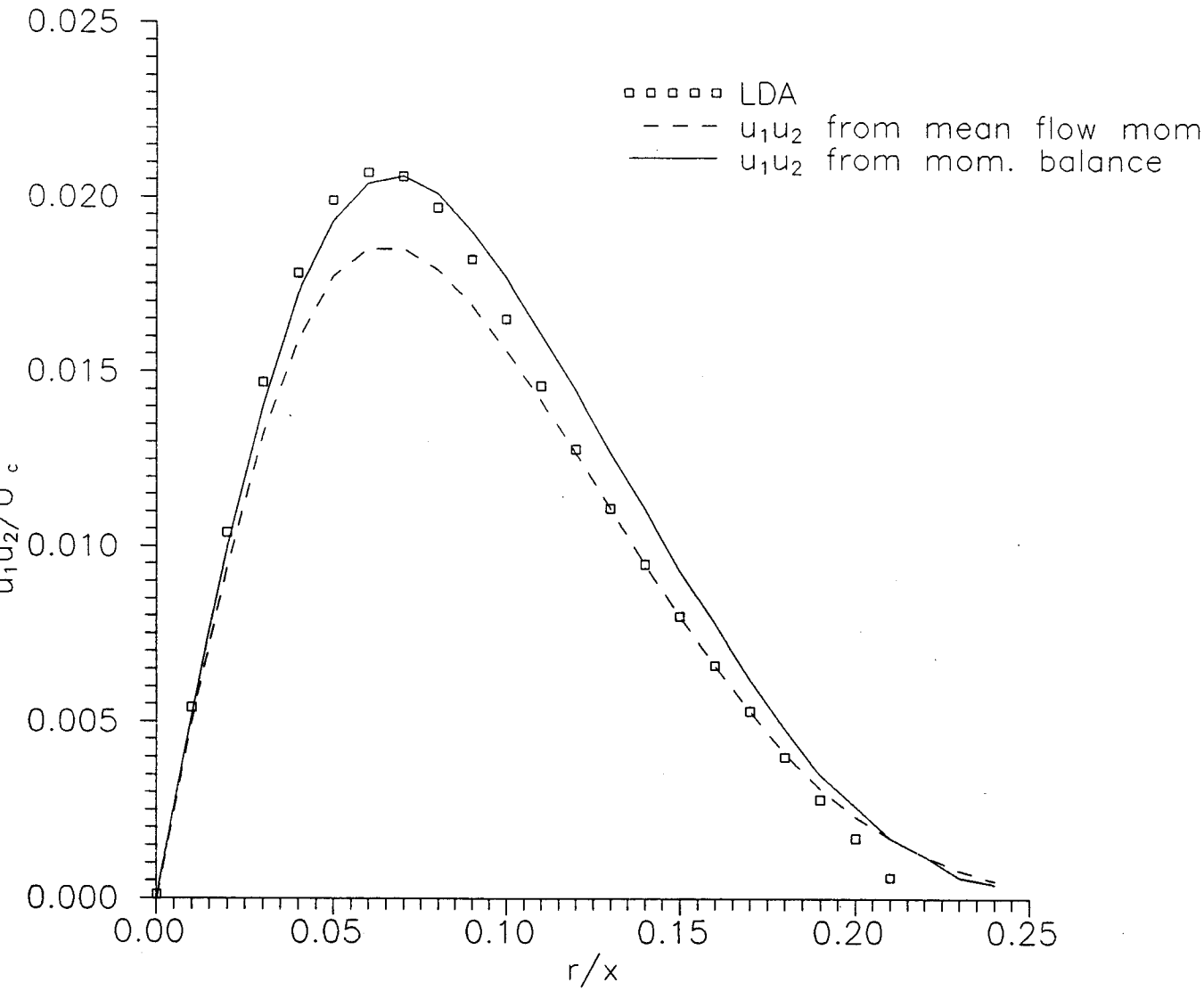

Figure 10. Turbulent Shear Stress, u_1u_2/U^2_c

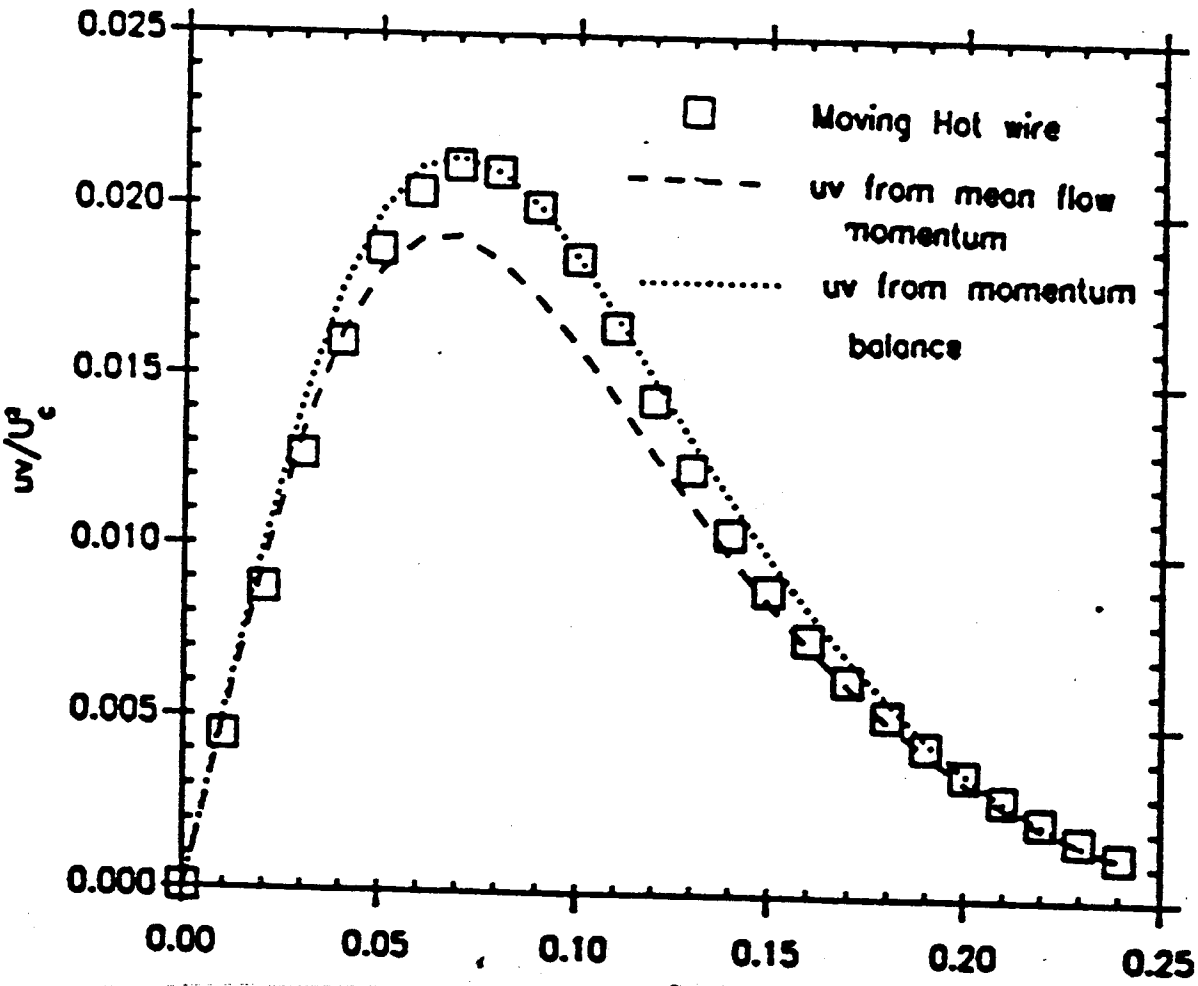

Figure 11. Prediction of Turbulent Shear Stress, Flying Hot Wire.

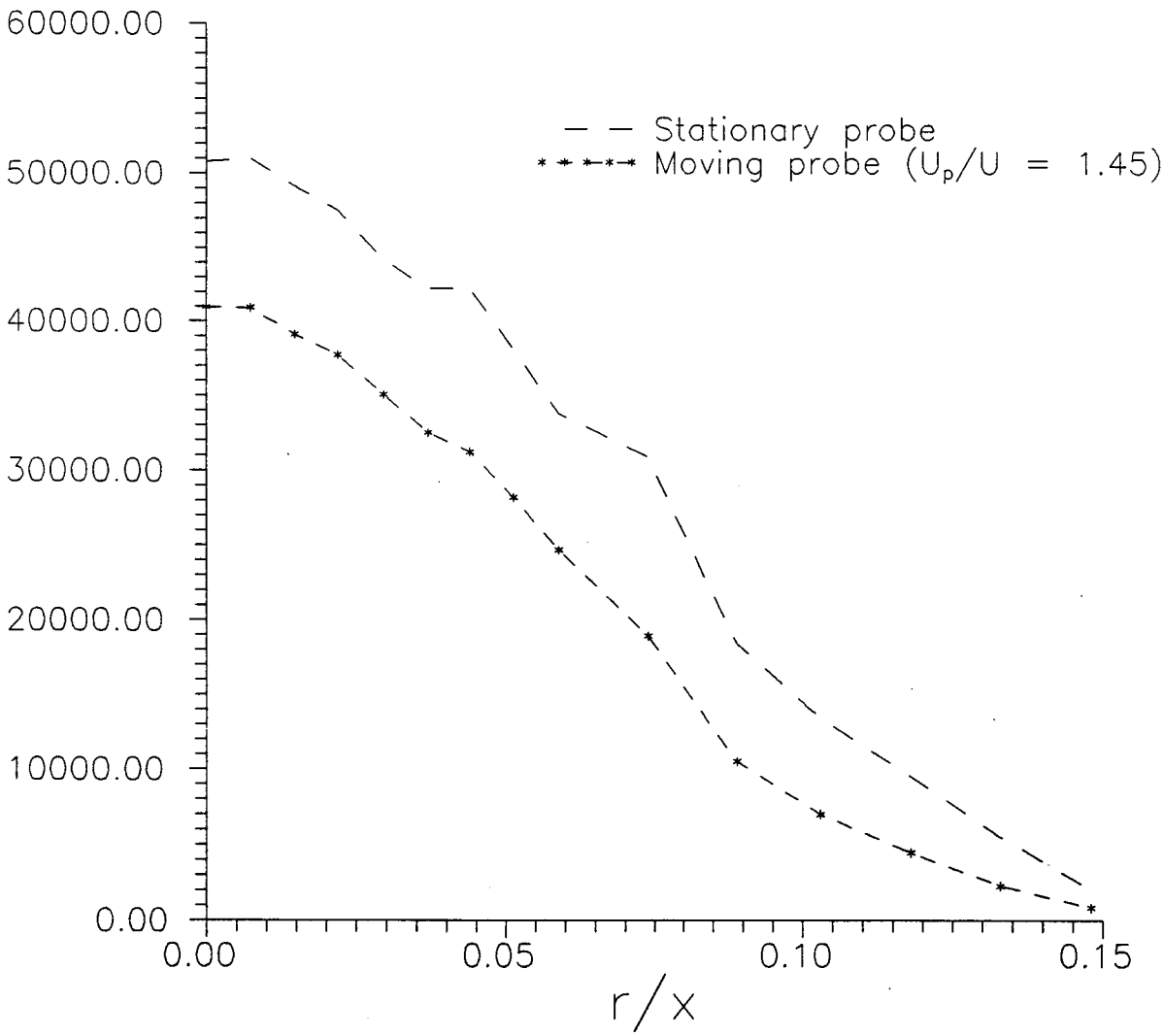

Figure 12. Measured mean square derivatives versus r/x

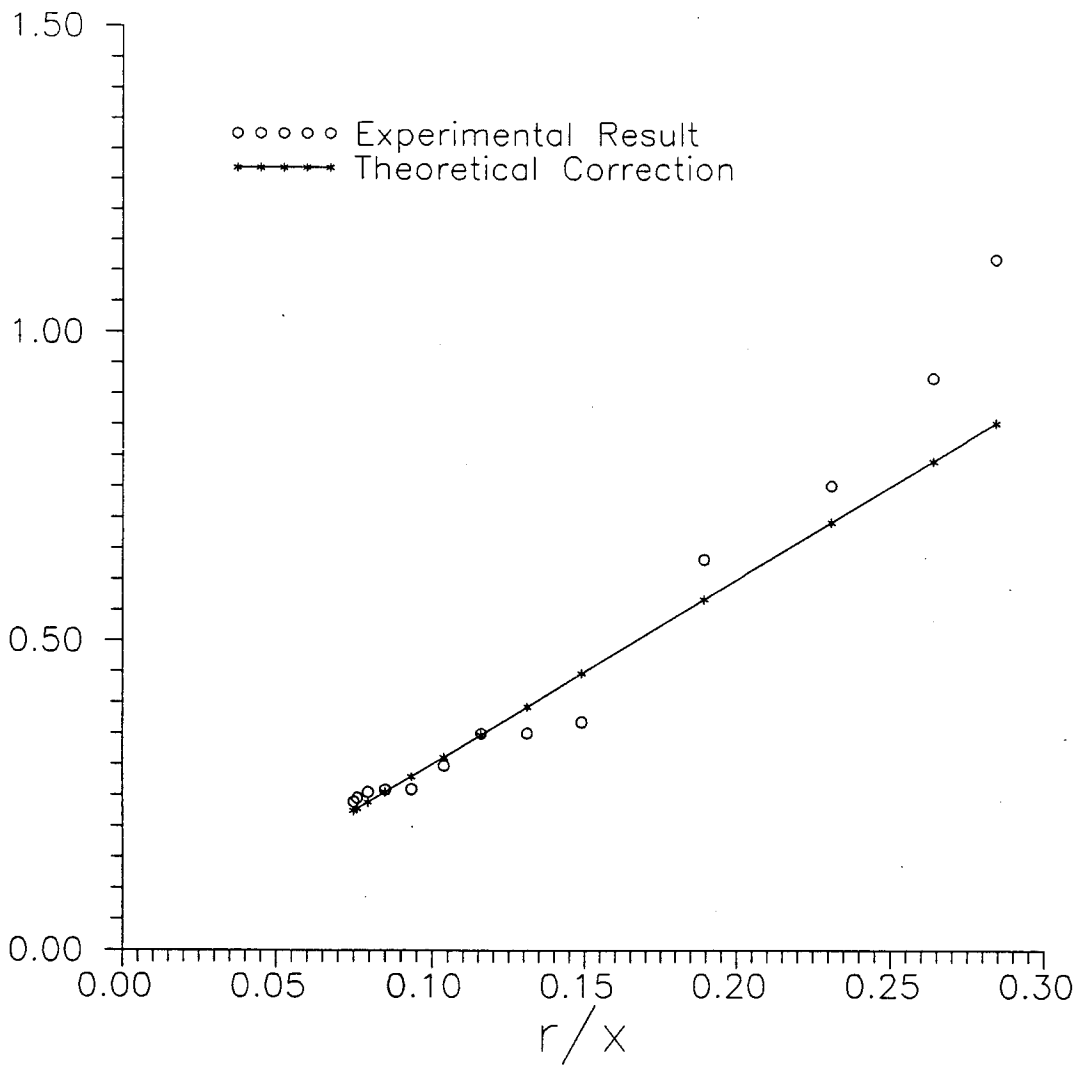
1.50
1.00
0.50
0.00
Experimental Result
Theoretical Correction
0.00
0.05
0.10
0.15
0.20
0.25
0.30
r/X

Figure 13.

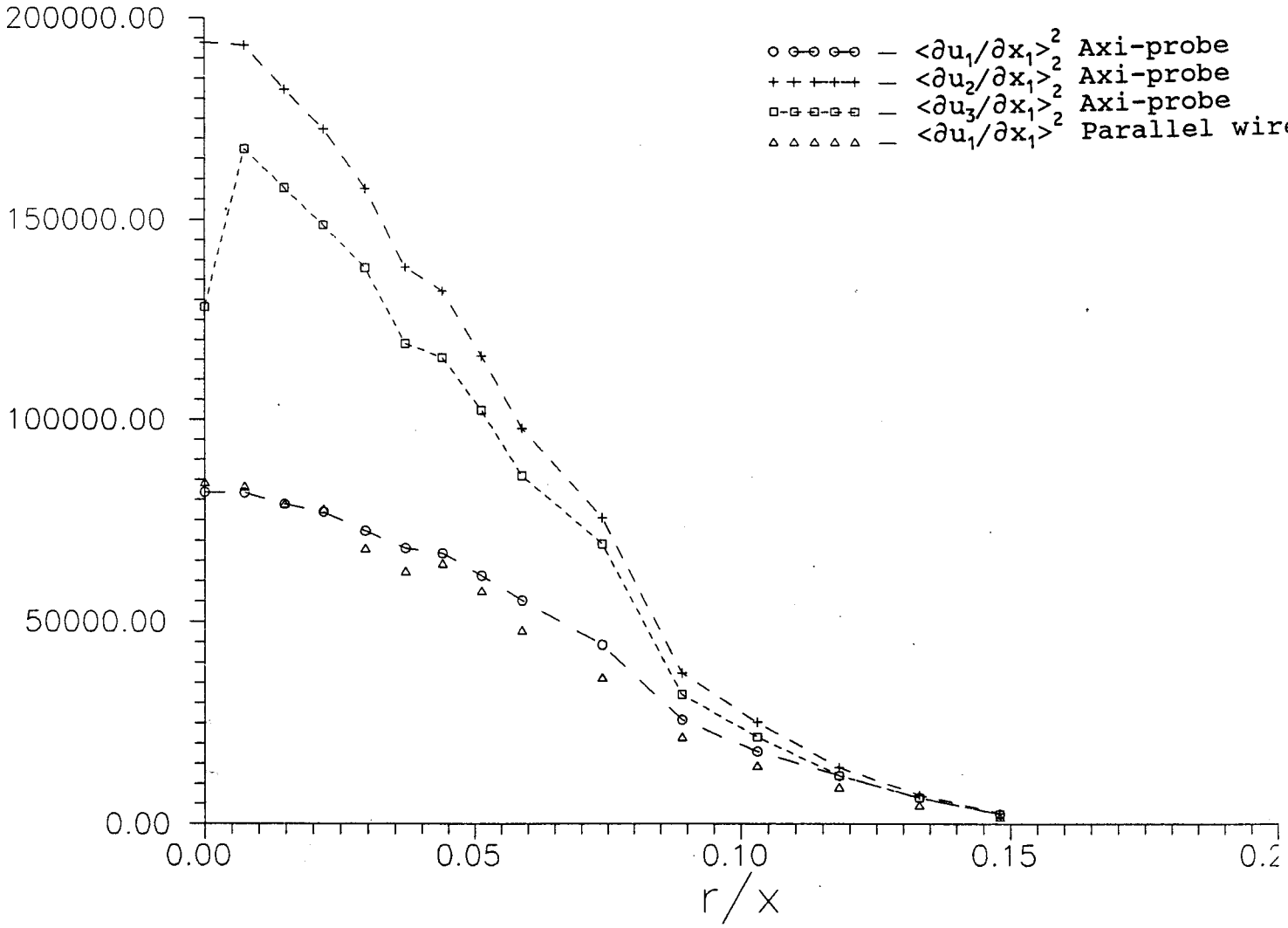

Figure 14. Derivative Correlation Coefficients in the Streamwise Directions

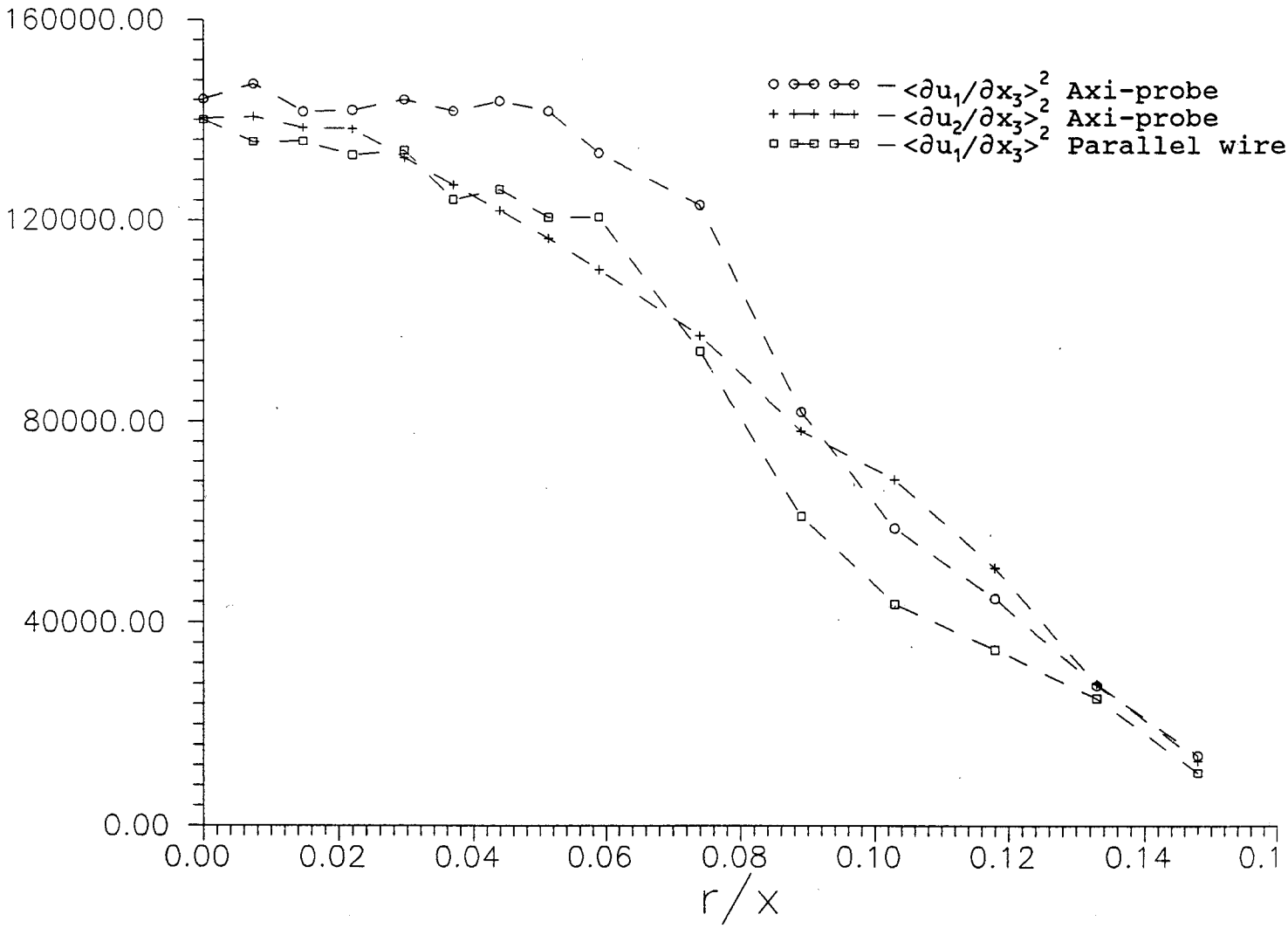

Figure 15. Derivative Correlation Coefficients in the Azimuthal Direction.

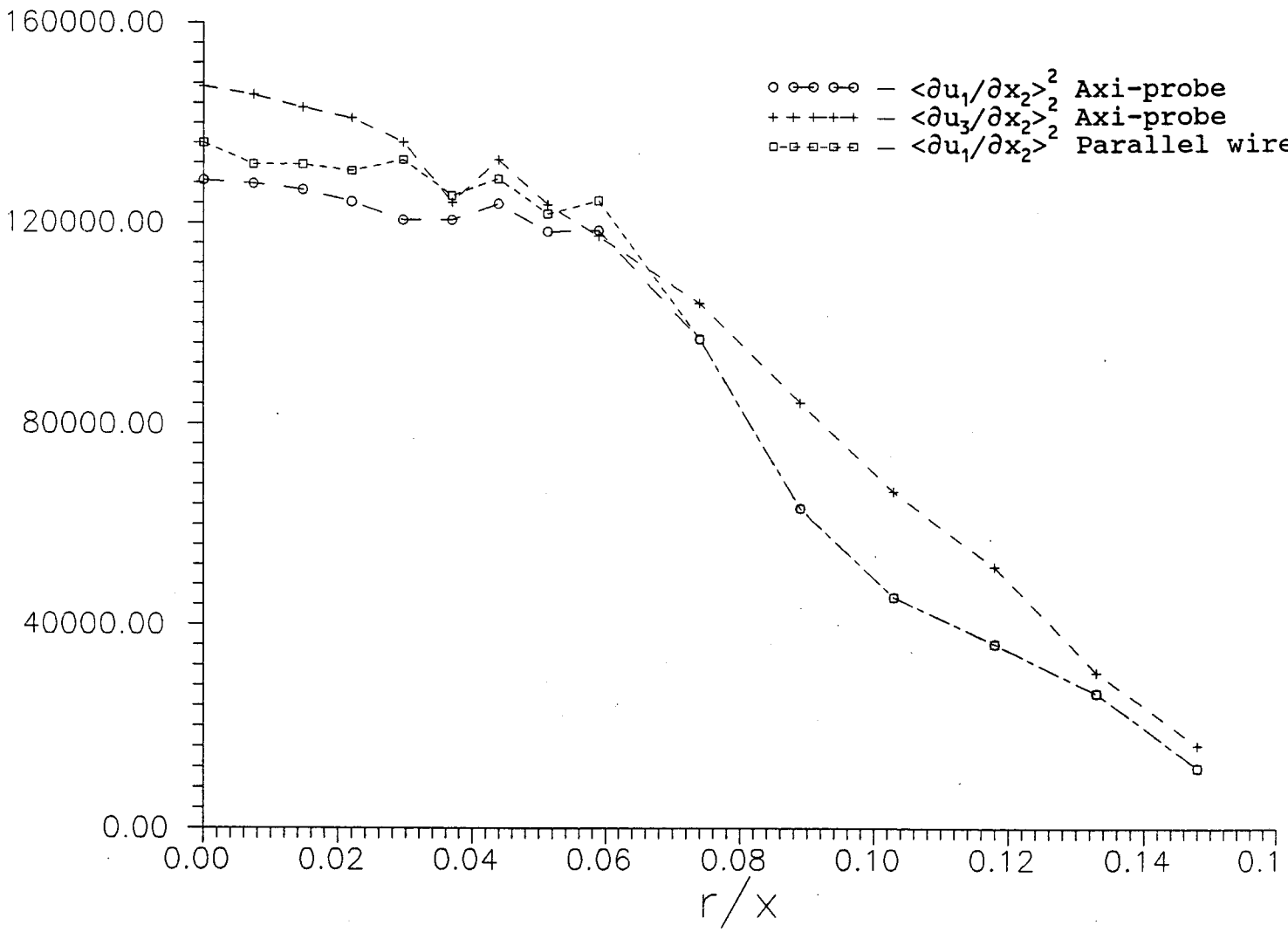

Figure 16. Derivative Correlation Coefficients in the Radial Direction.

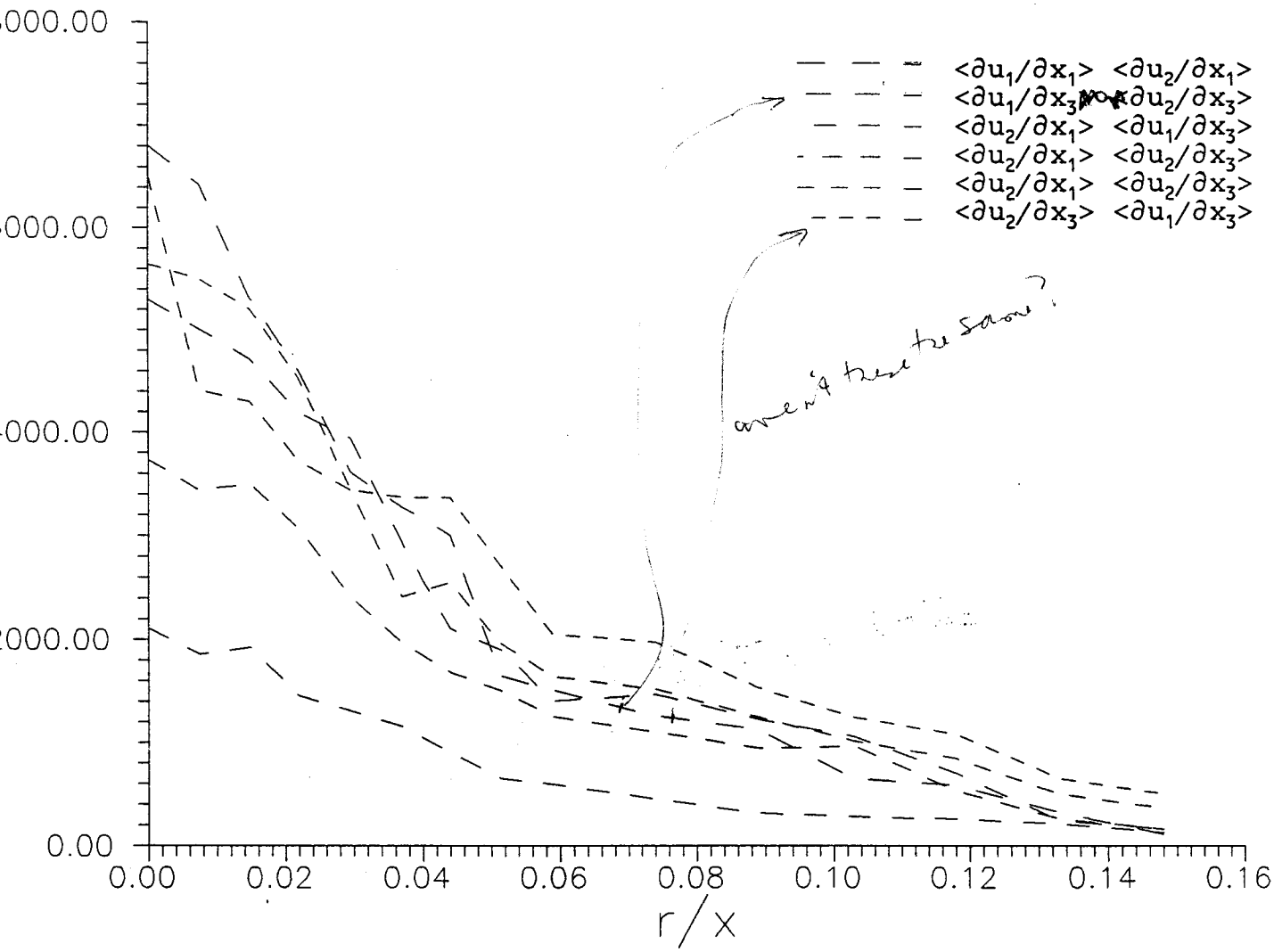

Figure 17. Derivative Correlation Cofficients

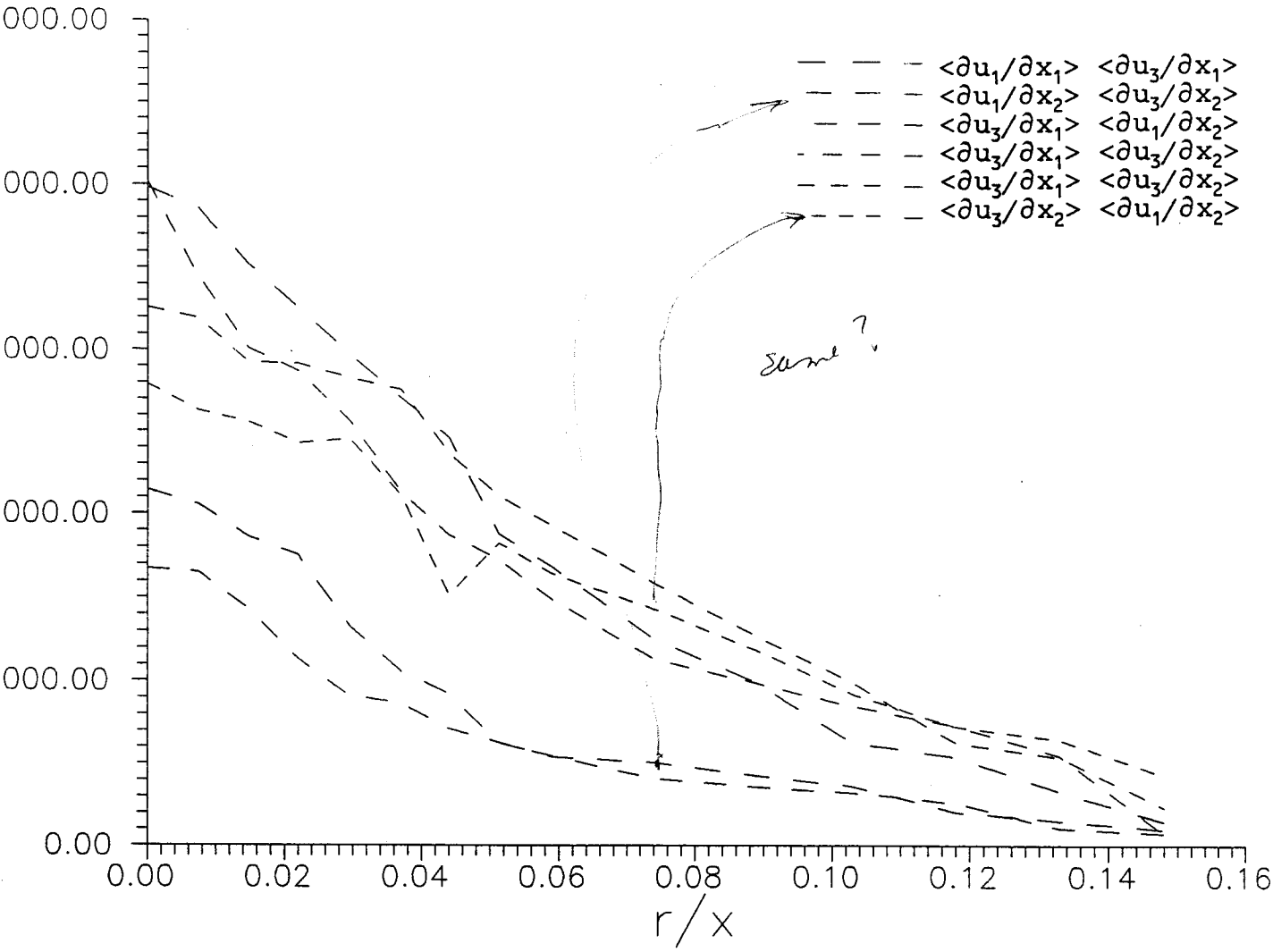

Figure 18. Derivative Correlation Cofficients

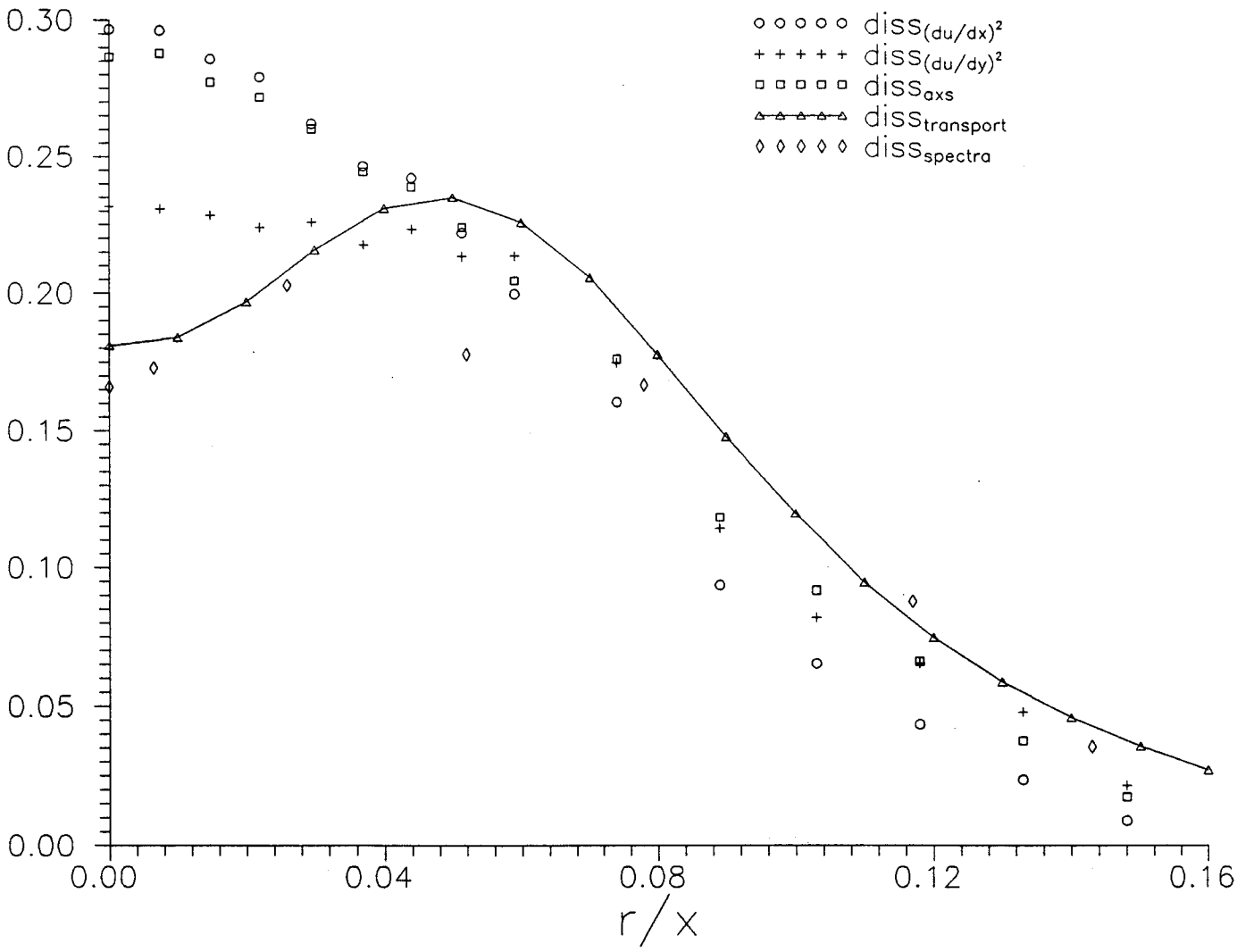

Figure 19. Disspation Profile